*metals*

MDPI

*Review*

# Fabrication Techniques and the Formation Mechanism of Nanoparticles and Nanoclusters in Metal Materials

**Junwei Qin [1], Xiaohua Chen [2,*], Yanlin Wang [1], Yuzhi Zhu [1], Shiwei Pan [2], Wei Zhou [1], Mingwen Chen [3] and Zidong Wang [1,*]**

[1] School of Material Science and Engineering, University of Science and Technology Beijing, Beijing 100083, China
[2] State Key Laboratory for Advanced Metals and Materials, University of Science and Technology Beijing, Beijing 100083, China
[3] School of Mathematics and Physics, University of Science and Technology Beijing, Beijing 100083, China
* Correspondence: chenxh@skl.ustb.edu.cn (X.C.); wangzd@mater.ustb.edu.cn (Z.W.)

**Abstract:** Continuous innovation in the design of metallic materials is essential for further progress in aerospace, automotive, construction, and shipping. Fine grain strengthening is considered to increase the strength of metals without losing plasticity. However, many fabrication techniques are restricted to very small sizes. Recently, the introduction of in situ nanoparticles with coherent or semi-coherent interfaces in the metallic matrix achieves simultaneous enhancement of the strength and ductility of metallic materials. In this review, the focus is on fabrication techniques and the formation mechanism of nanoparticles and nanoclusters in metal materials. The effects of nanoparticles on grain refinement, inhibiting segregation, second phase, and inclusion refinement are discussed, and the mechanism of simultaneous improvement in the strength and ductility of nanostructured metal materials is briefly covered. Finally, we provide a summary and outline of the possible direction for further advances in this research field.

**Keywords:** nanoparticles; coherent interface; metallic materials; strength; toughness



**Citation:** Qin, J.; Chen, X.; Wang, Y.; Zhu, Y.; Pan, S.; Zhou, W.; Chen, M.; Wang, Z. Fabrication Techniques and the Formation Mechanism of Nanoparticles and Nanoclusters in Metal Materials. *Metals* **2022**, *12*, 1420. https://doi.org/10.3390/met12091420

Academic Editor: Irina P. Semenova

Received: 31 July 2022
Accepted: 24 August 2022
Published: 28 August 2022



## 1. Introduction

Metallic materials have been used in aerospace, automotive, construction, and shipping due to their excellent strength and other requirements for formability, weldability, fatigue, resistance to fracture, corrosion, or wear resistance [1–6]. To meet the performance requirements of steel, copper, aluminum, and other metal materials in different application fields, it has been the pursuit of the researcher to improve comprehensive properties. As such, an advance in strength and ductility means the lightweight or service life improvement of components under the same application conditions and reducing the consumption of natural resources. In the future, metals will still be an irreplaceable material in social development. Therefore, increasing the strength of metals without sacrificing other properties is the development trend of metallic materials in the future [7,8]. However, improving strength often results in the decrease in other properties, such as ductility, toughness, conductivity, and corrosion resistance. Properties of metal material depends on microstructure of inclusion, second-phase, and grain size. At present, the industrial application of metal materials has the problems of microstructure inhomogeneity, such as coarse grain, serious segregation, coarse inclusions, and second phase. Solving the inhomogeneous microstructure is the key to achieving uniform properties of metal materials.

According to the Hall–Petch relationship [9], the strength is proportional to the reciprocal square root of the grain size. Fine grain strengthening is considered to be an important approach that increases the strength of metals without losing plasticity. A lot of effort has been paid to increasing the number of boundaries such as grain boundaries

and coherent twin boundaries. In general, the methods of grain refinement can be divided into metallurgical treatment refinement, severe plastic deformation (SPD), physical field method, and rapid solidification technique. Metallurgical treatment refinement is achieved by adding inoculants or modifiers to the metal melt, and it generally is intermetallic compounds or chemical elements. This method is usually easy to operate and has a remarkable refining effect, but it requires fine and dispersed inoculant to effectively refine the grains. Otherwise, it will affect the properties of the material. In addition, recent studies show that in situ particles can act as heterogeneous nucleation sites to realize grain refinement [10–12]. Ultrafine crystalline materials are produced by SPD, such as equal-channel angular extrusion (ECAE) [13–15], high-pressure torsion (HPT) [16,17], multi-axial compressions/forging (MAC/F) [18], accumulative back extrusion (ABE) [19,20], and accumulative roll-bonding (ARB) [21]. Nevertheless, when the grain size is full below ~1 μm, for ultrafine crystalline materials, strengthening is usually accompanied by a drop in conductivity and toughness [22]. In similar, gradient nanostructure (GNS) papered by surface severe plastic deformation (SSPD) is considered to be an effective means to optimize mechanical properties [23–25]. Surface mechanical attrition treatment (SMAT) [26,27], surface mechanical grinding treatment (SMGT) [28,29], and surface mechanical rolling treatment (SMRT) [30,31] were used to prepare GNS metals. In past decades, researchers apply physical fields or change heat transfer conditions during solidification to improve microstructure. Centrifugal casting, pulse current casting [32], ultrasonic vibration casting [33], pulsed magnetic field casting [34], die-casting, and squeeze-casting utilizes the interaction of the metal melt and the physical field to enhance the uniformity of the as-cast microstructure. However, the grain size is still large (about 100 μm). The rapid solidification technique refers to the alloy liquid to solid at an extremely fast solidification rate under a much faster cooling rate (up to 100 K/s) than conventional solidification. The extremely high cooling rate in additive manufacturing can result in significant grain refinement [35]. In addition, the atomization method [36,37], strip casting [38,39], and spray deposition are common rapid solidification methods, which are used to prepare powder, strip, and small-size bulk metal respectively, and these techniques are limited to size and shape. Therefore, there is still a problem in the engineering application and preparation of large nano and microcrystalline metal materials.

Metal matrix reinforced by secondary particles is another example of strengthening methodology. In general, for the secondary particles have an incoherent interface with the metal matrix, when interacting with dislocations, the dislocations cannot go through but block at these interfaces where a source of crack is produced with the dislocation pilling up, which inevitably leads to the decline of the ductility of the metal materials. Moreover, when the relationship between the precipitates and the matrix changed from coherent to semi-coherent or incoherent, the strength of the materials deteriorated gradually [40]. Hence, the enhancement effect of second phase strengthening not only relies on the size and distribution of particles but also on the wettability between the surface of particles and the metal matrix. Nanostructured materials have a better balance between strength and ductility than materials with nearly similar chemical compositions and different microstructures [41]. Nanostructured materials are generally composed of micron/submicron grains and nanoparticles or nanoclusters within grains. Some researchers reported that nanostructured materials exhibited a good combination of strength and ductility, which is mainly associated with the refinement of grain size and dispersed nanoparticles or nanoclusters.

The purpose of this review is to summarize the theoretical technologies on nanoparticles or nanoclusters formation in metal materials and to explore the optimization effects of in situ and ex situ nanoparticles on the microstructure and properties of metallic materials. Examples of nanoparticles and nanoclusters applications in steel, copper, and aluminum alloy are elaborately discussed in the fabrication techniques, microstructure, and mechanical properties. Mechanism of nanoparticles on grain refinement, inhibiting segregation, second phase, and inclusions refinement are discussed. The mechanism of simultaneously

improving the strength and ductility of nanostructured metal materials is briefly covered. Finally, we provide a summary and outline the possible direction for further advances in this research field.

## 2. Formation of Nanoparticles and Nanoclusters

Nanoparticles and nanoclusters can be divided into in situ and ex situ according to the different formation mechanisms and methods. In general, the in situ nanoparticles are formed or precipitated during the casting, hot rolling [42], and heat treatment [5,43–46]. The ex situ nanoparticles, through powder metallurgy [47], are introduced into molten metal via the master alloy [4,48,49] and additive manufacturing [11,50,51]. Here, a brief recap of the nanoparticles and nanoclusters formation mechanisms is given.

### *2.1. Formation Mechanism of In Situ Nanoparticles during Solidification*

During the solidification of the metal melt, the initial atomic group or crystal nucleus that forms nanoparticles are first formed from the melt, and the crystal nucleus is generally regarded as spherulite. In the past decade, Chen studied the particle growth in alloy melt induced by far-field uniform flow [52,53], straining flow [54–57], interfacial kinetics [58], shear flow [59], oscillatory flow [60], and anisotropic surface tension [61–63], and constructed a mathematical and physical model for the initial stage of crystal growth. By using the asymptotic method to find the compatible asymptotic solution to the model, these solutions show the interface velocity $U_1$ of crystal nucleus growth.

$$U_1 \approx \frac{dR_0}{dt} + \varepsilon\frac{dR_T}{dt} + \alpha_4\frac{\partial R_{aniso}}{\partial t} + \varepsilon\frac{\partial R_{uniform}}{\partial t} + \varepsilon\frac{\partial R_{streaming}}{\partial t} + \varepsilon\frac{\partial R_{shear}}{\partial t} \quad (1)$$

where $R_0$ is leading order approximations of the crystal-melt interface shape; $\varepsilon$ is a dimensionless relative undercooling parameter; $\alpha_4$ is the anisotropy parameter; $R_T$ is the crystal-melt interface shape affected by the temperature and concentration change; $R_{aniso}$ is the contribution of the anisotropic surface tension to the crystal-melt interface shape; $R_{uniform}$, $R_{streaming}$, and $\partial R_{shear}$ is the crystal-melt interface shape affected by far-field uniform flow, linear straining flow, and shear flow, respectively. In addition, $dR_0/dt$ is the interface velocity of crystal nucleus growth without external files and describer as:

$$\frac{dR_0}{dt} = \frac{M_s}{100M_m r}\frac{\rho_m}{\rho_s}D_L(C_L - C_e) \quad (2)$$

where $r$ is the diameter of the crystal nucleus; $D_L$ is the solute diffusion coefficient in liquid metal; $\rho$ is the density; $M$ is the molecular weight; $C_L$ is the solute concentration in the front of the interface; $C_e$ is the equilibrium solute concentration of the crystal nucleus; $m$ is the alloy element; and $s$ is the crystal nucleus. According to Equation (2), it can be found that the growth speed of the crystal nucleus had a positive correlation with the solute micro area concentration in the front of the interface, growth speed can be controlled by adjusting solute concentration in the front of the interface. Since the size of particle nucleation in the melt is generally at the nanometer level, the growth speed of the nanoparticle is reduced to zero, with the decrease of the solute content in the front of the interface. A large number of nanoparticles are obtained in liquid metal.

In short, the formation of nanoparticles in the metal melt can be achieved by changing the interface anisotropic, controlling solute content in the front of the interface, and introducing various flow fields such as shear flow.

For in situ nanoparticle steel, a new method to generate nanoparticles in a liquid melt before casting is by controlling solute content in the front of the interface [64]. This method is named multipoint dispersion supply technology in the smelting process, and a schematic diagram of the method is shown in Figure 1. Firstly, the pure Ti wire added in the melt is multipoint dispersion, and the free-state oxygen [O] concentration should be controlled within several ten ppm. Secondly, the convection field is formed in the melt by electromagnetic stirring or Ar bottom blowing, which promotes the flow of the molten

metal. With this process, Ti will react with oxygen and a large number of titanium oxide homogeneous nucleation cores are formed. Finally, the melt was poured into the casting mold with an air-cooling rate, and nanoparticles are dispersed homogeneously inside the steel casting ingot. This method is applied in the subsequent development of high-strength low-alloy (HSLA) and weld metals to improve microstructure and properties [10,64–71], such as optimizing inclusions and refining grains and enhancing strength without losing plasticity to resistant stress corrosion cracking.

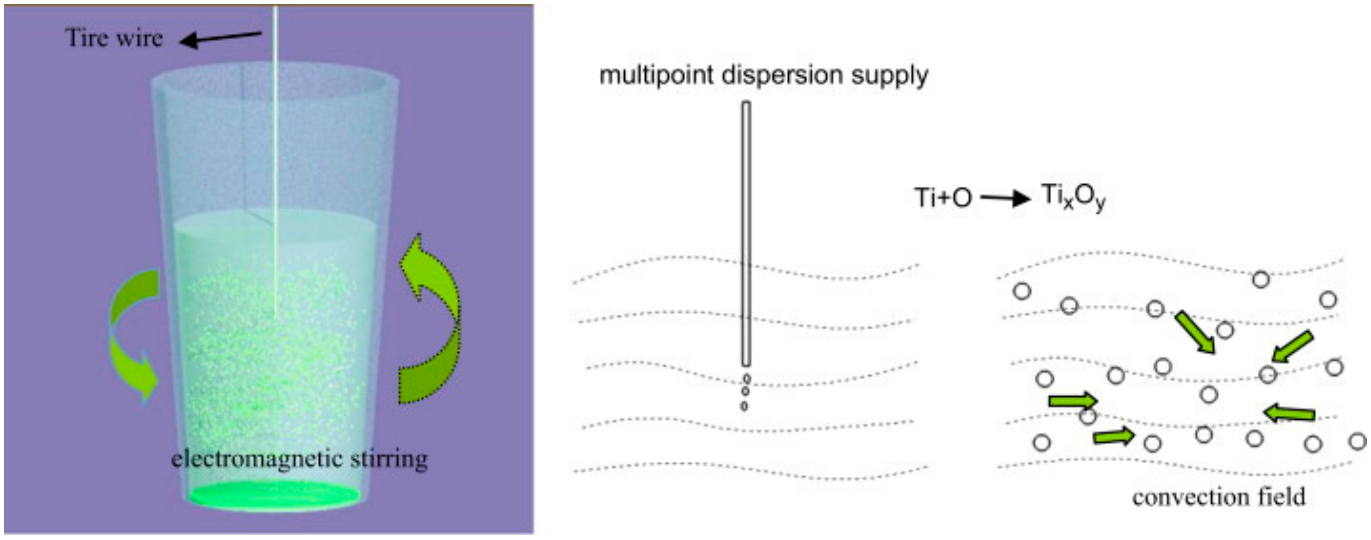


**Figure 1.** Schematic of the processing method for the formation of nanoparticles in melt through a combination of multipoint dispersion supply method and electromagnetic stirring, reprinted with permission from ref. [64], 2022, Elsevier.

For in situ nanoparticle copper alloy, we first started the investigation on Cu-3Sn-8Zn-6Pb alloy [72], which fabricates copper alloys reinforced with in situ nanoparticles by centrifugal casting in a vacuum chamber. On this foundation, Cu-10Sn-2Zn-1.5Fe alloy [73], single crystal Cu-Fe alloy [74], Cu-10Sn-2Zn-(1-3) Fe-0.5Co alloy [75–79], Cu-(1-3) Fe-0.5Co alloy [80–84], and Cu-12Sn-1.5Ni-(0-1.5)Fe alloy [3,85] was fabrication and investigation. Figure 2 shows a schematic diagram of NPFG structure preparation technology for tin bronze alloy. In it, Fe or Co raw materials were added to the melt and all atoms are uniformly distributed with induction heating. Then, iron-rich nanoparticles are in situ generated, which as potent adsorption/nucleation are the core formation of the Cu adsorption layer. In the end, grain nucleation occurs stochastically on the nanoparticles and copper melt solidification as nanoparticle-fine grain (NPFG) structure by centrifugal casting. According to the previous study [72], when the iron clusters in the copper melt are greater than 0.37–0.58 nm, the nucleating growth begins, and the growth rate is in large values ($10^2$–$10^3$ m $s^{-1}$). With a large growth rate, it is very difficult to obtain the dispersed iron nanoparticles in a copper matrix melt during solidification. Under this condition, the introduction of shear flow into the copper melt by centrifugal casting can significantly reduce the growth rate of iron nanoparticles and control the size of nanoparticles. The role of nanoparticles has been confirmed, such as heterogeneous nucleation [77], inhibiting segregation [78], and enhanced combination of strength and ductility [74,76].

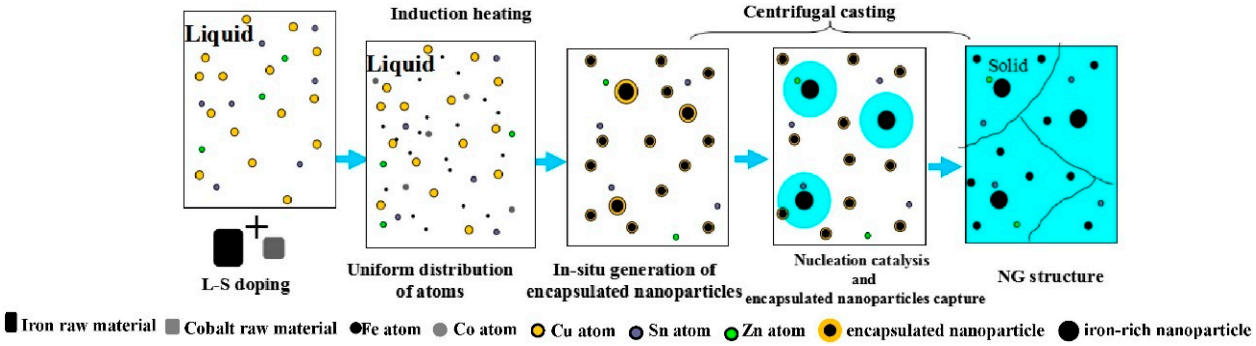


**Figure 2.** Schematic diagram of NPFG structure in situ formed in cast Cu-10Sn-2Zn-1.5Fe-0.5Co (wt.%) alloy, reprinted with permission from ref. [76], 2022, Elsevier.

### *2.2. Formation of In Situ Nanoparticles during Deformation and Heat Treatment*

There are a high number density precipitation of fine nanoparticles in the metallic matrix by thermomechanical processing and controlled heat treatment, which strengthened the matrix while still maintaining good ductility and formability. In general, the precipitation in the process of metal thermal deformation and heat treatment is a complex transformation, but it can be simply understood as two steps: solid solution and aging precipitation.

Taking steel, for example, heat treatment involves: (1) annealing at 800–1000 °C to form a homogeneous full austenite structure, (2) cooling to room temperature at a certain cooling rate, so that all the austenite is transformed into ferrite (including martensite), and (3) multiple aging treatment is applied to cause corresponding precipitation. The type of precipitates is closely related to alloying elements and matrix structure. Microalloying elements, such as Nb, V, and Ti, were added to transformation-induced-plasticity (TRIP) steels [86], quenching and tempering (Q&T) steels [42], and ferritic steels for precipitation strengthening. Copper is used to increase strength in steel processed by aging treatment, via forming Cu-rich nanoparticles [45,86–88]. In addition, the main elements of maraging steel and maraging stainless steels are Ni and Cr, respectively, and other alloying elements could be Al, Ti, Si, Mn, and Mo. Various precipitates tend to form in the early stage of aging, such as η phase ($Ni_3Ti$, $Ni_3Mo$) [89], B2 phase (Ni (Al, Mn, Ti)) [44,90], Laves phase ($Fe_2Mo$) [90], and G phase ($M_6X_{16}Si_7$) [91,92]. The ferritic steel results in the primary form of precipitates being carbides, and fine precipitation in ferrite is mainly formed in two stages: (1) interphase precipitation (IP) formed during the transformation from austenite to ferrite, which is usually manifested as rows of very fine particles in austenite-ferrite interface [93,94], and (2) at aging stage of ferrite as homogeneously or heterogeneously distributed random precipitation (RP) [45,86]. The strength of bainitic steel is mainly related to its microstructure, such as the thickness of bainitic ferrite (BF), solid solution strength of BF, dislocation density of BF, and precipitation in BF. Alloy carbides could precipitate in bainite on isothermal hold, slow cooling, or on holding after the finish of bainite transformation [93,95]. The austenite transforms into martensite, when the cooling rate from austenitizing temperature is fast enough, and martensite is a metastable supersaturated solid solution (carbon and other substitutional alloying elements). In the early stage before martensite tempering, the clusters of interstitial carbon atoms are randomly distributed in the martensite matrix [96]. Most martensite steels improve toughness by tempering, which is accompanied by the spinodal decomposition of martensite and precipitation of carbide. In recent years, the strength and impact toughness of martensite steel have been enhanced by the precipitation of fine alloy carbides for secondary hardening. The ultra-high strength maraging steel, upon aging nanosized intermetallic precipitation, occurs leading to high strength levels [44,88–90] that have attracted continuing attention.

Precipitation-strengthened copper alloy is required to simultaneously possess high strength, excellent electrical conductivity, and ductility. According to previous studies [97], nanoparticles are dispersed on the pure copper matrix, and maintain a spacing of more

than 45 nm, which can avoid the electron scattering effect of the precipitation and enable the copper alloy to obtain a combination of strength and conductivity. A larger number of studies have been devoted to regulating the microstructure and precipitation behavior of precipitation-strengthened copper alloy by mechanical and aging treatment processes. Deformation-induced defects improved the precipitation and the number density of precipitates and composition optimization measures such as type and contents of alloying elements. In general, Cu-Fe-P alloy, Cu-Ni-Si alloy [5,98–100], and Cu-Cr alloy [101,102] were mainly precipitated fcc-Fe, $Ni_2Si$, and bcc-Cr, respectively. Furthermore, multi-precipitation phases of $Ni_3Si$, $Ni_3Al$, $Cr_3Si$, $Co_2Si$ [40,102], and $Cu_4Ti$ [102,103] were precipitated during the aging process of multicomponent copper alloy.

The diffusion mechanism is widely accepted as the precipitation nucleation mechanism of aluminum alloys. The number density and size of spherical nano precipitates, such as $Al_3Sc$, are affected by the supersaturation of the aluminum matrix and aging temperature. In the temperature range of 673~713 K, the coarsening behavior of $Al_3Sc$ precipitates in the Al-0.2 wt% Sc alloy can be divided into coherent stage, coherent/semi-coherent coexistence stage, and semi-coherent stage [104]. The diffusion mechanism cannot explain the difficulty of nucleation of precipitates which is completely coherent with the matrix, such as the T1 phase in Al-Cu-Li alloy [105]. In addition, the micro-alloying method is widely used to adjust the precipitation behavior of nano-size strengthening precipitates to further improve the mechanical properties of age-hardening aluminum alloys. The effect of trace amounts of alloying elements on the precipitation behavior of age-hardened aluminum alloys can be divided into four main aspects: promoting precipitation [46,106], segregating to interface between precipitates and $\alpha$-Al matrix [107], changing types of precipitated phases, and creating extra strengthening dispersoids [46,107].

### *2.3. Technology of Introducing Ex Situ Nanoparticles into Metallic Materials*

Additive manufacturing (AM), powder metallurgy by mechanical alloying, and introduction into molten metal via the master alloy are the most common methods for adding ex situ nanoparticles into metallic materials.

AM is adept at producing complex geometries and can be optimized for lower weight and enhanced capabilities. In this process, providing a high density of heterogeneous nucleation nanoparticles ahead of the solidification front promotes a fine equiaxed grain structure to achieve fine grain strengthening and dispersion strengthening at the same time [51,108]. This technology can be divided into two parts [11,50,109]. Firstly, the nanoparticles and metal powder are fabricated by various methods, such as inert gas atomization and mechanical milling. Secondly, a machine spreads a layer of powder onto a built plate and then locally melts a specific layer of powder material by a selective laser. This process is shown in Figure 3 [11]. According to previous study [50], laser-based AM technologies need to solve at least three problems: (1) in most cases, the added ex situ particles (diameter $\leq$ 5 μm) would deteriorate the flowability of the matrix powder; (2) due to the difference of laser absorptivity, the heat input between ex situ particles and metals is different, which complicates the melting and solidification process; and (3) the wettability of the metal matrix and ex situ particles is difficult to control.

Before the method of introducing molten metal via the master alloy is adopted, the traditional method of directly adding nanoparticles into molten metal has some problems, such as the large difference between the specific gravities of the particles and molten metal, non-uniform dispersion of particles [110], and contamination of particle surface. The researchers solved the above problems by adding master alloy into the metal melt, and the specific process is as follows: (1) the nanoparticles prepared in a master alloy by self-propagating high-temperature synthesis (SHS, Figure 4a–c) [48], stir-casting method [49], and powder compact method [111]; (2) the metal melt was poured into a casting ladle with the pre-fabricated nanoparticle master alloy (Figure 4d,e) [48], or master alloy was added into the molten metal and stirring treatment [49]; (3) and the nanoparticles were uniformly dispersed in the metal matrix during the tumbling of the molten metal(Figure 4f,g). This

method could solve non-uniform dispersion and segregation problems arising from the difference in specific gravity between the nanoparticles and the matrix.

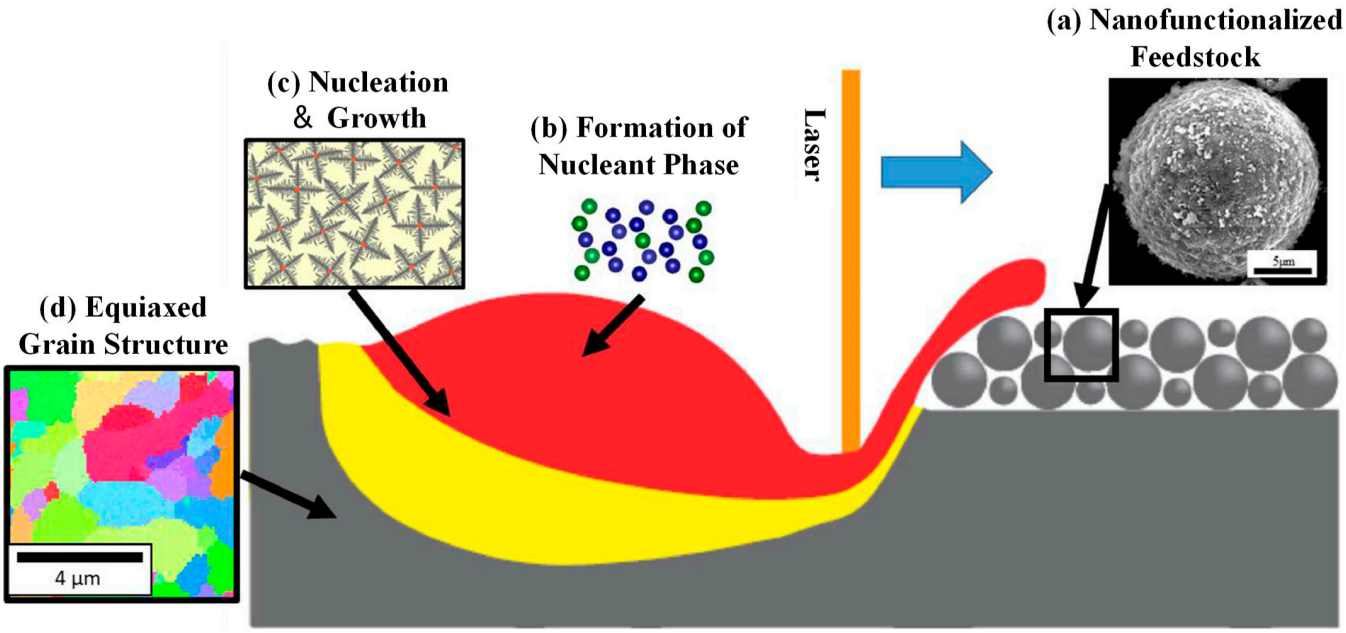


**Figure 3.** Process of laser-based additive manufacturing with nanoparticles and metal powders. Laser scan left to right, (**a**) nanoparticles and metal powders, (**b**) formation of nucleate in the melt, (**c**) promoting heterogeneous nucleating, and (**d**) leading to an equiaxed final microstructure in the printed part, reprinted with permission from ref. [11], 2022, Elsevier.

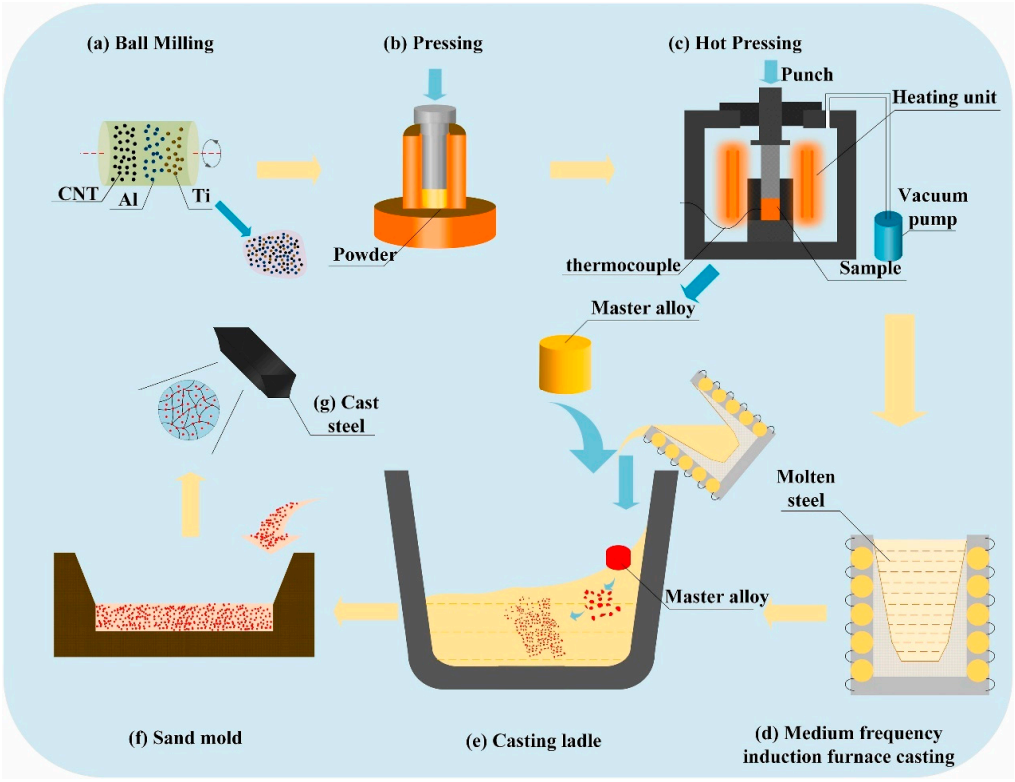


**Figure 4.** Schematic of the preparation process of the 40Cr steel manipulated by trace TiC nanoparticles, reprinted with permission from ref. [48]. 2022, Elsevier.

Oxide dispersion strengthened (ODS) steel is the most representative metal material containing ex situ nanoparticles prepared by powder metallurgy [47], the manufacturing process involving mechanical alloying, consolidation techniques and thermal/mechanical treatments. The mixed powders of pure metal and nanoparticle (nanosized yttrium oxide-$Y_2O_3$) were mechanically alloyed by a ball mill. Then, hot isostatic pressing [47], hot extrusion [112], and spark plasma sintering [113,114] are commonly used to consolidate the mechanically alloyed powders. Finally, machining and thermal treatments according to the application requirements of the components. Figure 5 shows a series of manufacturing processes of fuel cladding that is 8.5 mm in diameter by 0.5 mm in thickness by 2 m in length [115].

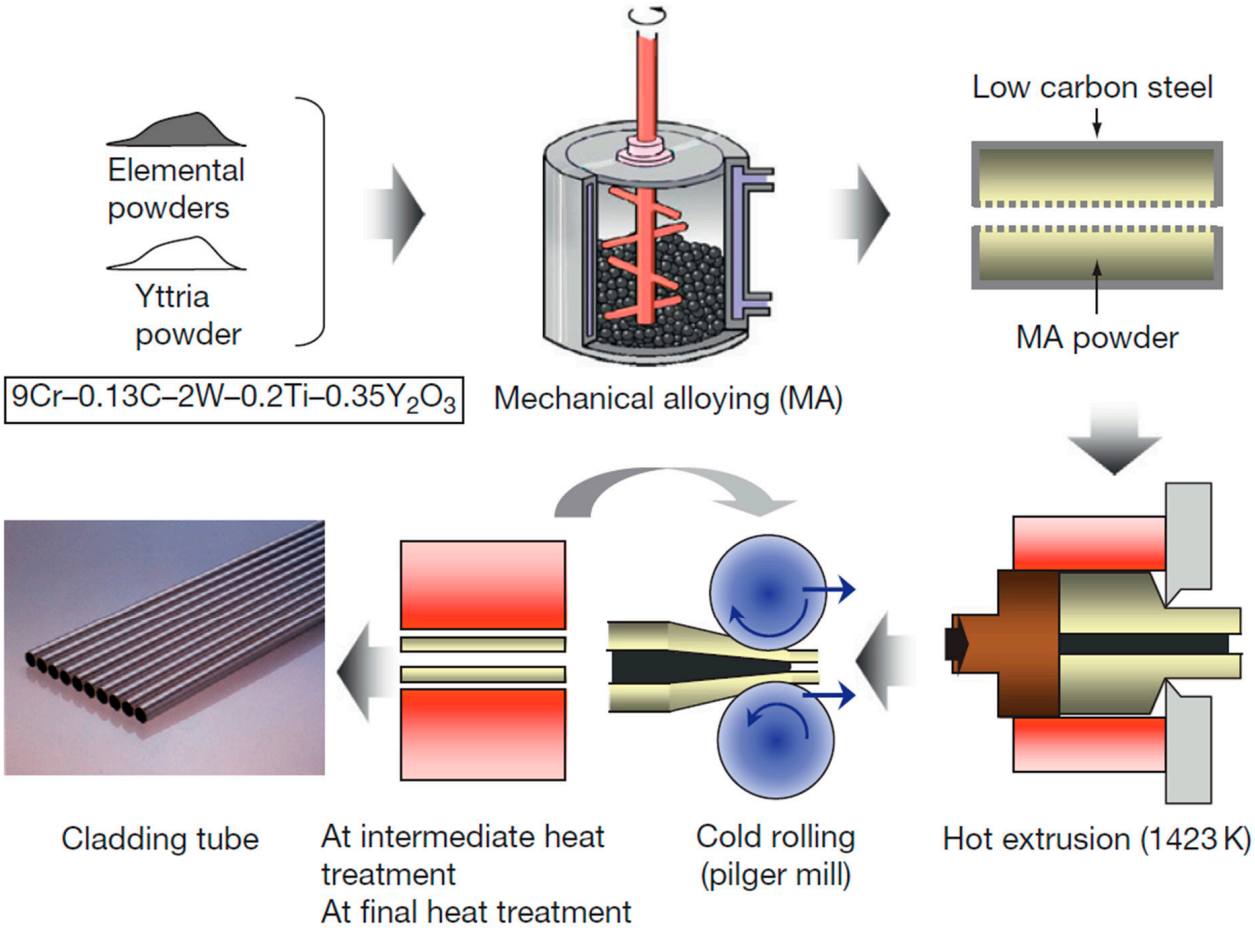


**Figure 5.** Schematic of powder metallurgy by mechanical alloying manufacturing processes of cladding tube reprinted with permission from ref. [115], 2022, Elsevier.

## 3. Optimization of Microstructure

### *3.1. Grain Refinement*

The grain refinement in previous studies is mainly due to the heterogeneous nucleation effect of nanoparticles. In particular, heterogeneous nucleation induced by in situ nanoparticles can produce a strong grain refinement effect, and in situ nanoparticles have uniform distribution and excellent wettability with alloy matrix. A series of fabricated metals by in situ nanoparticles reinforcement technology have achieved grain refinement, such as hot rolled Q195 [64], tin bronze [77], and Ni-Cr-Mo HSLA [69]. In addition, heterogeneous nucleation can be achieved by introducing ex situ nanoparticles into the metal melt through mechanical alloying and master alloy, such as twin-roll casting Al-Cu strips [4], nano-treated AA7075 [110], and ODS steel [109,114]. Several morphologies of grain refinement are shown in Figure 6.

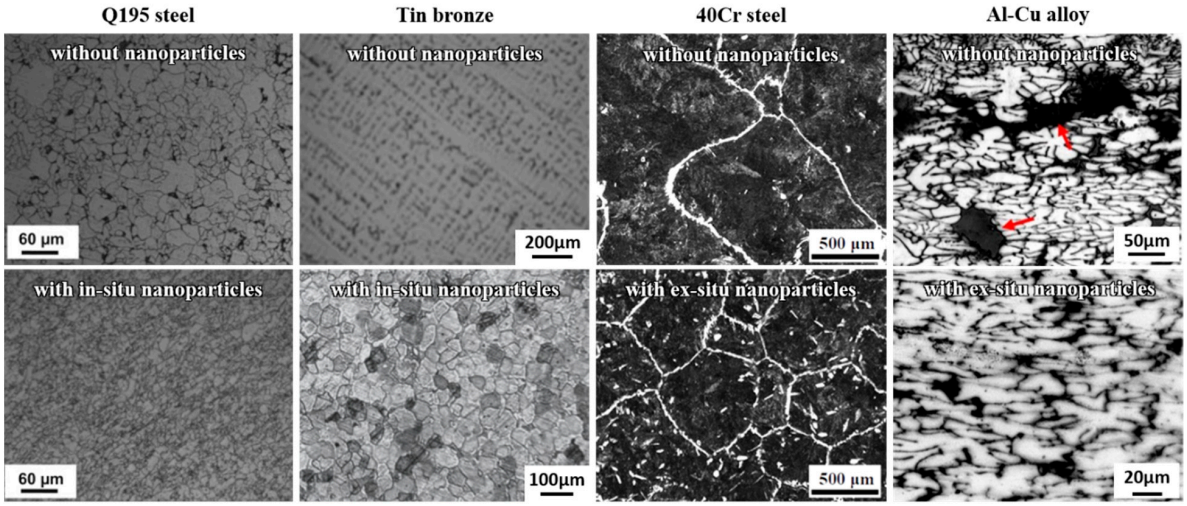


**Figure 6.** Grain refinement effect caused by nanoparticles in hot rolled Q195 steel, reprinted with permission from ref. [64]. 2022, Elsevie.; tin bronze, reprinted with permission from ref. [77]. 2022, Elsevie; 40Cr steel, reprinted with permission from ref. [48]. 2022, Elsevier, and Al-Cu alloy (The discontinuous black areas marked with red arrows are macro-segregation), reprinted with permission from ref. [4]. 2022, Elsevier.

Figure 7 shows a schematic diagram of microstructure refining mechanism by nanoparticles [116]. The refined grains caused by in situ and ex situ nanoparticles could be owed to the following factors [4,48,77]: (1) some trace nanoparticles were used as heterogeneous nucleation sites for matrix during solidification, promoting the nucleation process and refining the primary grain; (2) the other particles, which did not serve as heterogeneous nucleation sites, were absorbed onto the solid-liquid interface, thereby restraining the growth of dendrites [49]; (3) nanoparticles providing more nucleation sites for recrystallization after deformation; (4) in subsequent heat treatment, the ex situ nanoparticles could induce the Zener pinning effect on the grain boundaries and hindering grain growth. In addition, in steel, nanoparticles provided heterogeneous nucleation sites for proeutectoid ferrite during the phase transition. The morphology of ferrite changed from strip growth along the primary grain boundary to a granular shape.

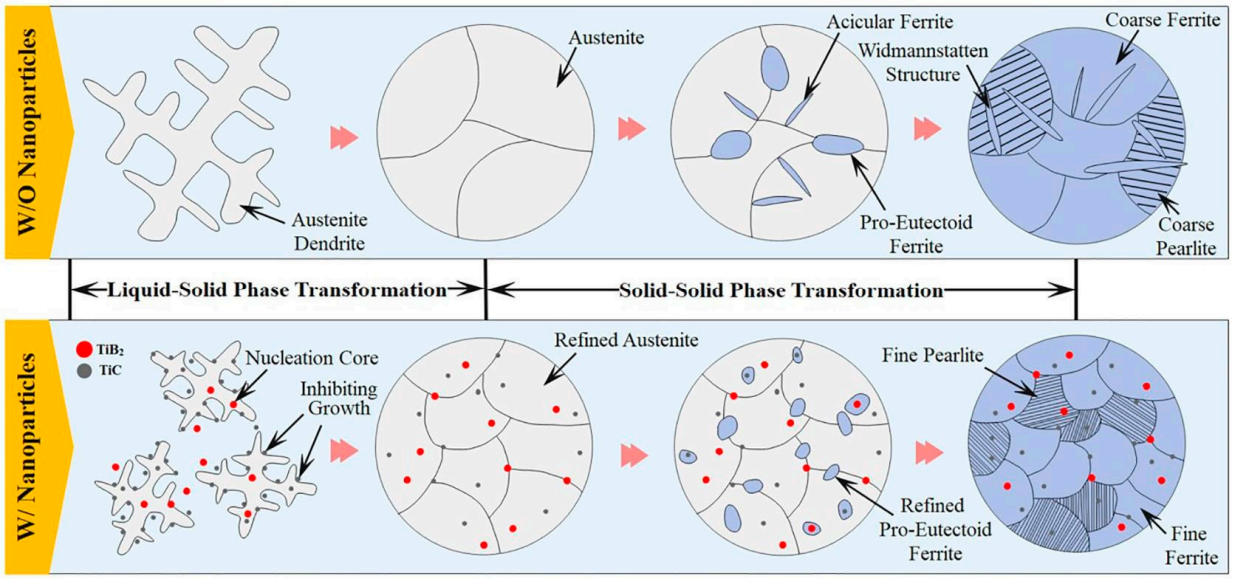


**Figure 7.** Microstructure refining mechanism by nanoparticles, reprinted with permission from ref. [116], 2022, Elsevier.

### *3.2. Inhibiting Segregation*

Homogenization of alloying element composition is a prerequisite for homogenization of metal structure. Previous studies show that the addition of nanoparticles can inhibit segregation, and the result is shown in Figure 8. Compared with the original as-cast microstructure, the segregation phase of tin bronze alloy with trace Fe and Co elements is obviously reduced [73]. The main difference between the two alloys is that a large number of dispersed iron-rich nanoparticles are formed in the tin bronze alloy with Fe and Co elements; the in situ nanoparticles eliminate segregation [3,81]. Liu et al. [4] fabricate Al-5Cu and Ti/C Al-5Cu strips by vertical-type twin-roll casting. The center macro-segregation of the Al-Cu strip was well mitigated by the addition of TiC nanoparticles, and the segregation band was replaced by a few Cu-rich phases discontinuously distribution in the inter-dendrite/grain zone with a narrow range.

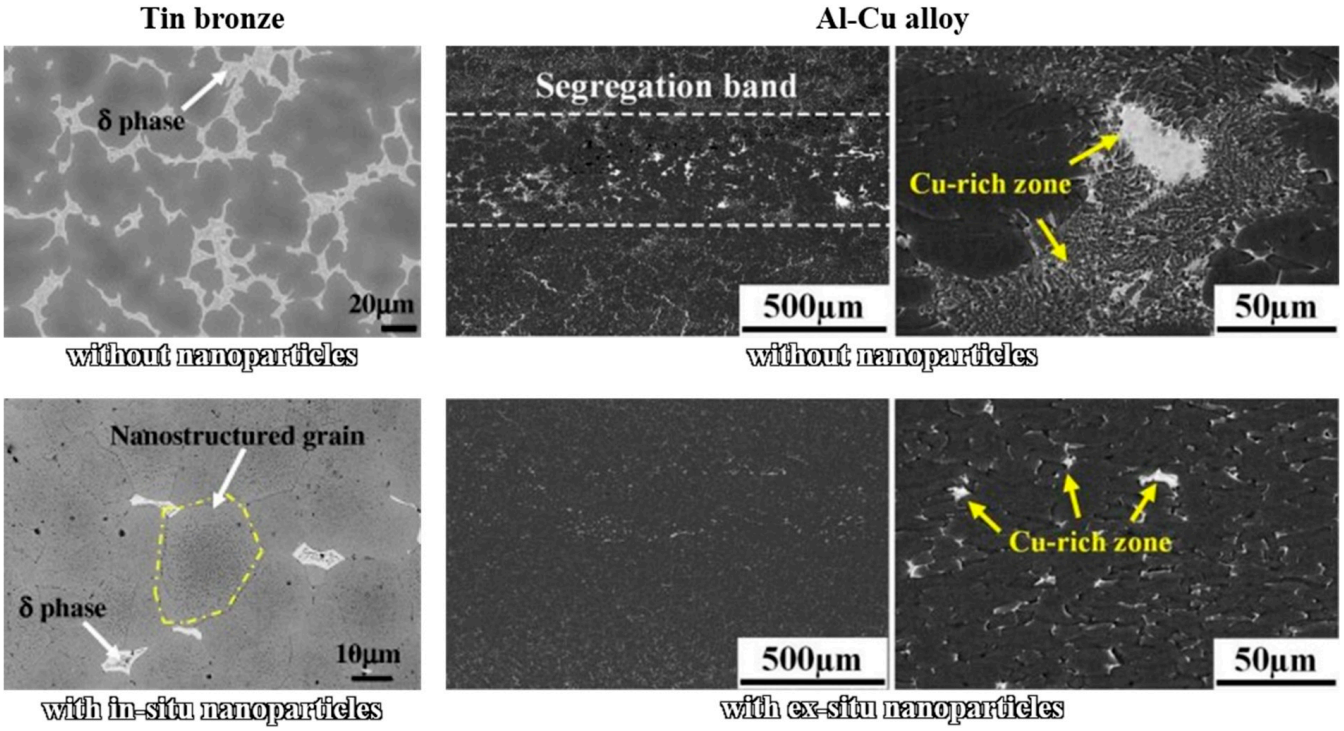


**Figure 8.** Inhibiting segregation caused by nanoparticles in tin bronze (δ phase and nanostructured grain are marked by white arrows), reprinted with permission from ref. [73], 2022, Elsevier, Al-Cu alloy strip (Cu-rich zone are marked by yellow arrows), reprinted with permission from ref. [4], 2022, Elsevier.

Chen et al. [78] describe the mechanism of iron-rich nanoparticles near S/L interface absorbing Sn atoms and blocking Sn atoms from escaping from S/L interface; a schematic diagram is shown in Figure 9. During the solidification, in situ nanoparticles consisting of Fe and Co precipitate in the melt prior to copper solidification, and they build an in situ nanoparticles wall near S/L interface due to high distribution density. With copper grain growing, low-melting-point Sn and Zn atoms released from S/L interface and diffuse into liquid. They conduct irregular Brownian motion with in situ nanoparticles in the melt. Sn and Zn atoms absorb at the surface of nanoparticles (situation I) or bounce off into S/L interface (situation III, IV). Finally, tin segregation is inhibited by iron-rich nanoparticles wall in a tin bronze alloy. Therefore, the introduction of nanoparticles into metal materials provides a feasible and practical method to eliminate segregation, which is expected to be applied to bulk metal materials to reduce segregation.

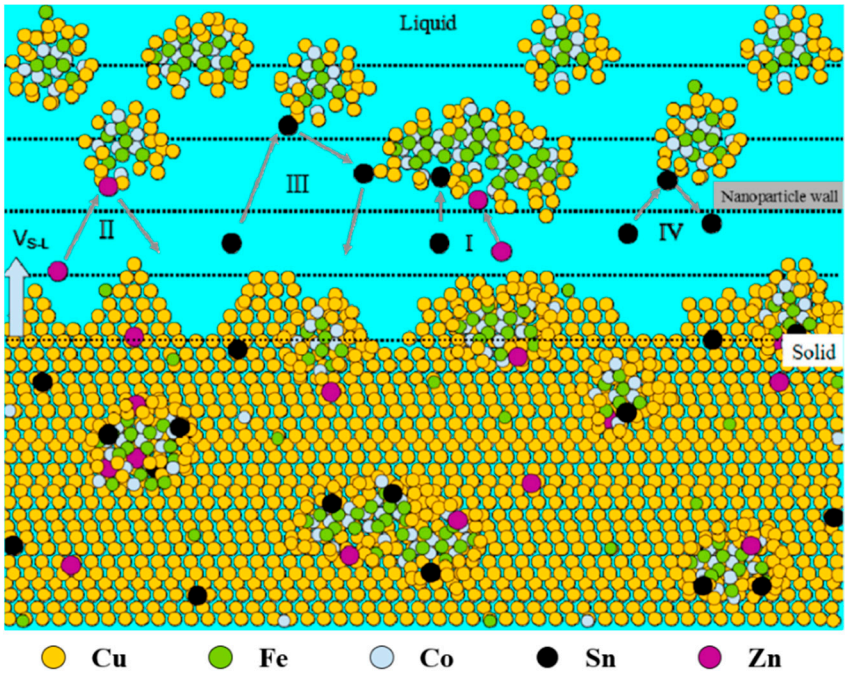


**Figure 9.** Schematic diagram of inhibiting Sn segregation by densely distributing iron-rich nanoparticles near solid/liquid interface (situation I: Sn and Zn atoms are absorbed on the surface of nanoparticles; situation II: Sn and Zn atoms encountered with the nanoparticles rebounded; situation III, IV: the rebounded Sn atoms are captured by advancing the S/L interface.), reprinted with permission from ref. [74], 2022, Elsevier.

### *3.3. Refinement of Second Phases and Inclusions*

Large-size inclusions and the second phase in metallic materials are important factors affecting their properties. Inclusions and second phase refinement, and conducting coherent/semi-coherent interfaces between particles and matrix, are considered to be effective means to optimize the properties of metallic materials [71,74]. The method of tailoring precipitation behavior of nano-sized strengthening precipitates by micro-alloying to improve the mechanical properties of age-hardening alloys has been widely used. The addition of alloying elements, such as Cd, Sn, and Ag, has a strong binding ability with vacancies and the Al element in Al-Cu alloy and an early stage of aging rapidly precipitate or form cluster, which greatly improves the precipitation strengthening. For example, Al-7Si-4Cu alloy with 0.28 wt.% Cd addition has a finer and denser microstructure of θ′ compared with Cd-free alloy [106], and pre-precipitation of Cd-rich particles has a heterogeneous nucleation effect on θ′ precipitates. Similarly, Er [46], Zr [107], and La [117] are added into the aluminum alloy to refine grain and precipitates. In addition, nanoparticles were obtained by designing the components of Al-$Al_3X$ peritectic, and $Al_3Ta$ intermetallic compounds have substantial grain-refining capacity under AM conditions [11]. The nanoparticle additions serve to alter the composition and microstructure, such as the change in the θ′ precipitate size [49]. Figure 10 shows a TEM micrograph of the refinement second phase in aluminum alloy.

Primary and secondary precipitates were obtained and refined from precipitation-strengthened copper alloys by multiple deformation and aging/annealing treatments [98,100,101]. The precipitates of two-stage cold rolling and aging treatment of Cu-Ni-Si alloy treated by pro-aging are refined from 120 nm to 60 nm [98]. Large deformation cold rolling promotes the precipitation of uniform and fine Ni2Si phase in C70250 copper alloy during aging, which improves the strength without damaging the conductivity [99]. According to previous studies, the orientation relationship between the precipitates and Cu matrix was $(001)_{Cu}$ //$(001)_{Cr}$ //$(001)_{Ni_2Si}$, $[011]_{Cu}$ //$[011]_{Cr}$ //$[010]_{Ni_2Si}$ [102,103]. Figure 11

shows TEM micrograph of refined precipitates and the orientation relationship between the precipitates and Cu matrix, respectively.

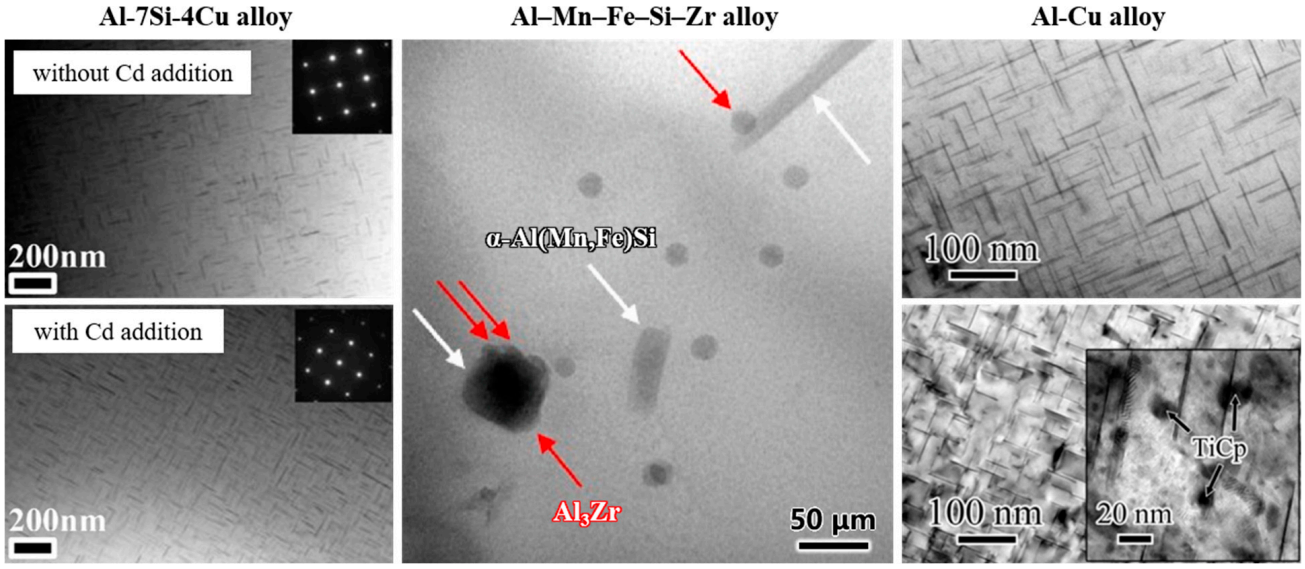


**Figure 10.** TEM micrograph of second phases in Al-7Si-4Cu alloy, reprinted with permission from ref. [106]. 2022, Elsevier; Al-Mn-Fe-Si alloy ($Al_3Zr$ and α-Al(Mn, Fe)Si are marked by red and white arrows, respectively), reprinted with permission from ref. [107]. 2022, Elsevier; Al-Cu alloy, reprinted with permission from ref. [49]. 2022, Elsevier.

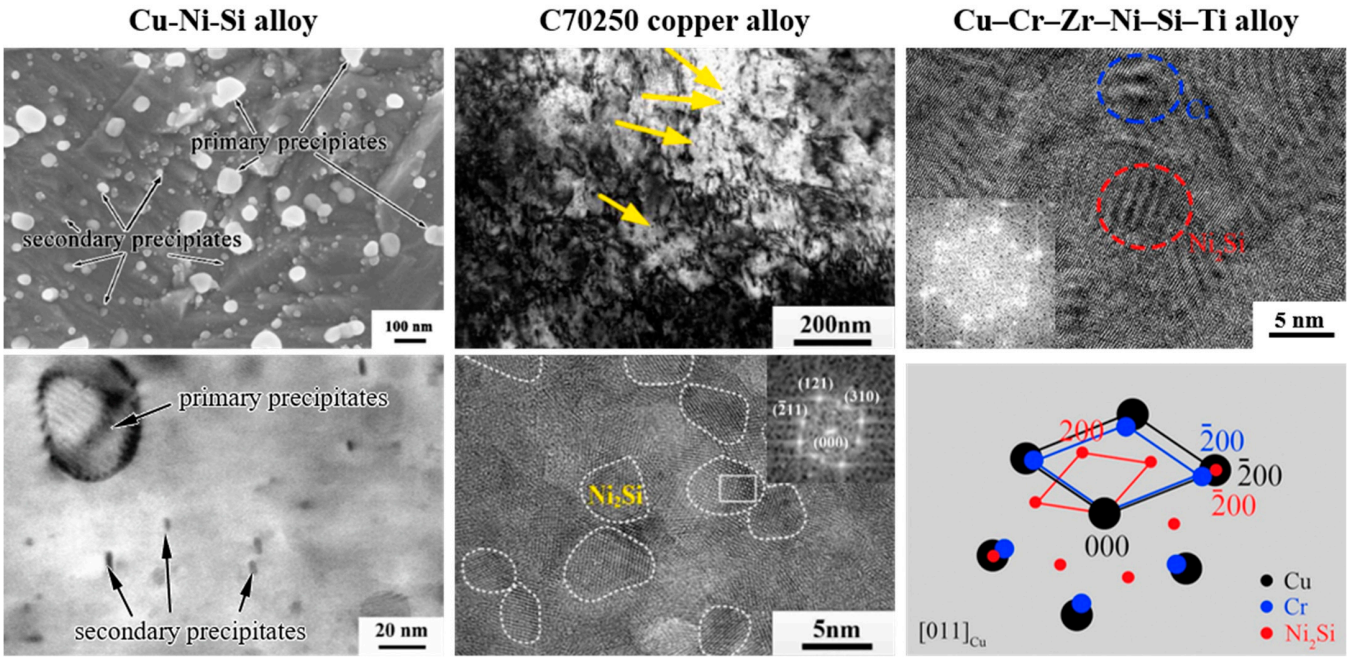


**Figure 11.** The micrograph of refined precipitates and the orientation relationship between the precipitates and the Cu matrix in Cu-Ni-Si alloy, reprinted with permission from ref. [98], 2022, Elsevier; C70250 alloy ($Ni_2Si$ phase is marked by yellow arrows, and the Fast Fourier Transform (FFT) diffraction pattern of $Ni_2Si$ in white square), reprinted with permission from ref. [99], 2022, Elsevier; and Cu-Cr-Zr-Ni-Si-Ti alloy, respectively, reprinted with permission from ref. [101], 2022, Elsevier.

The shape, size, and distribution of inclusions in steel have an important influence on the microstructure, micrograph, and mechanism properties. The nano/ micron inclusion in steel can be realized by multipoint dispersion supply technology [12,64,69]. The

principle of this technology follows: (1) Al and Ti compound twisted wires into the melt to obtain a high number of densities of in situ endogenous nanoparticles of $Ti_3O_5$ and $Al_2O_3$; (2) during the solidification process, MnS grew with $Al_2O_3$ as the core and form spherical or elliptical MnS-$Al_2O_3$ complex inclusion (1~2 μm) (Figure 12a) [10]; (3) during the tempering process, the Nb(C,N) precipitation grew with the $Ti_3O_5$ core and precipitates with the $Ti_3O_5$-Nb(C,N) core-shell structure (Figure 12b) [12]. Figure 12c shows a schematic diagram of the trace element multipoint dispersion supply method that refines inclusions and second phases [10].

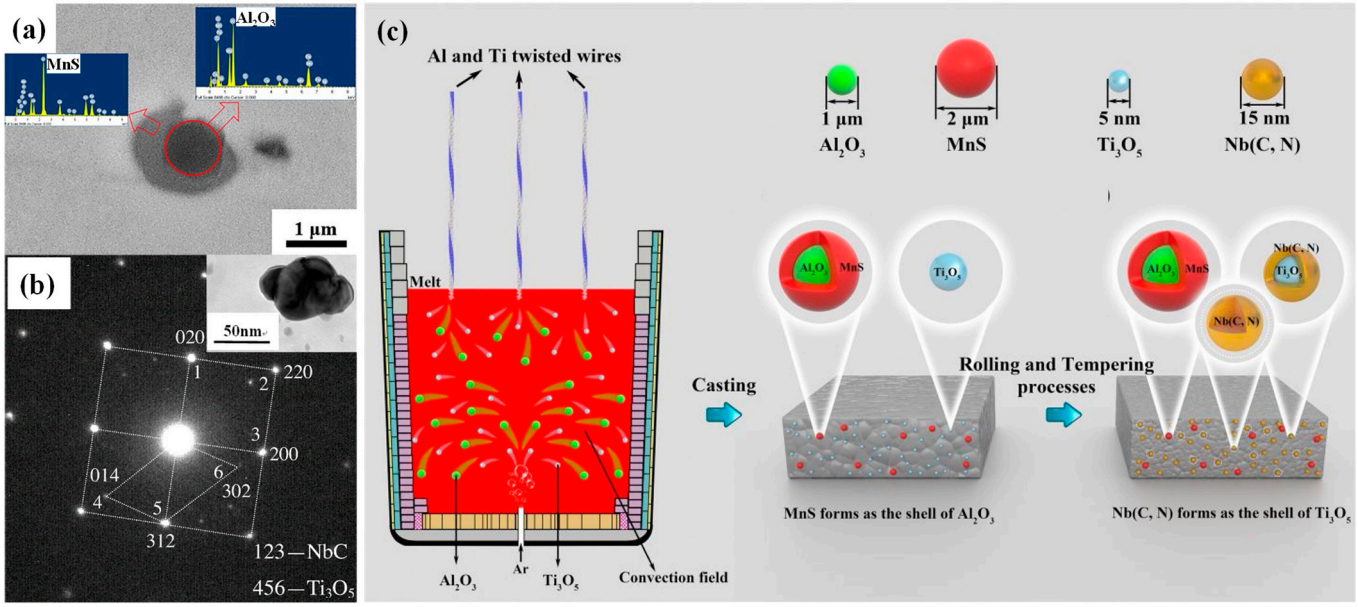


**Figure 12.** (**a**) SEM morphology of MnS-$Al_2O_3$ complex inclusion, reprinted with permission from ref. [10], 2022, Elsevier; (**b**) Index of SADP and TEM morphology of the $Ti_3O_5$-Nb(C,N) core-shell structure, reprinted with permission from ref. [10], 2022, Elsevier; (**c**) Schematic of the trace element multipoint dispersion supply method and the microstructure evolution in casting and tempering process, reprinted with permission from ref. [10], 2022, Elsevier.

## 4. Enhancement of Mechanical Properties

For metal alloys, the way to strengthen is by blocking the motion of dislocations in the matrix to obtain a high density of dislocation, while the increase of ductility depends largely on the long-term slip of the dislocation. Increasing dislocation density while avoiding dislocation pile-up is an important mechanism to realize the synergistic improvement of strength and plasticity of metal materials. A previous study shows that the hardening and softening of metallic during deformation are associated with the increase of dislocation density and the formation of local deformed zones with micro defects, respectively [118]. The improvement of mechanical properties by microstructure optimization is comprehensive, and the mechanical properties can be improved under static load [116,119], cyclic load [118,120], and shock load [48,87,119] conditions. For example, the dynamic non-equilibrium process (DPN) realized by impact-oscillatory loading significantly improves the plastic properties of two-phase high-strength fine-grained titanium alloys at room temperature [118]. In addition, as shown in Figure 13, it is reflected in the result of static load tensile tests at room temperature. He et al. [48] add trace TiC nanoparticles into 40Cr steel by master alloy to refine grain and homogenize microstructure; their strength and toughness were improved simultaneously. It can be attributed to fine grain strengthening, thermal mismatch strengthening, and second phase strengthening. Doping Cd into Al-7Si-4Cu alloy to optimize microstructure and properties, strength and ductility were simultaneously dramatically improved by larger number density and less size of θ′ precipitates [106]. Cai et.al [42] found that the multi-strengthening contribution of fine martensite laths, higher dislocation density,

and nano-precipitates in nano-precipitation strengthened ultra-low carbon (NPS—ULC). Ti–Mo–Nb steel can increase yield stress and without sacrificing tensile ductility. According to Gao et al. [45], in dual-phase (DP) steels, the combined contribution of the ultrafine microstructure, martensite volume fraction, grain orientation, and nano-sized Cu-rich precipitates is the underlying basis for the high strength and good ductility.

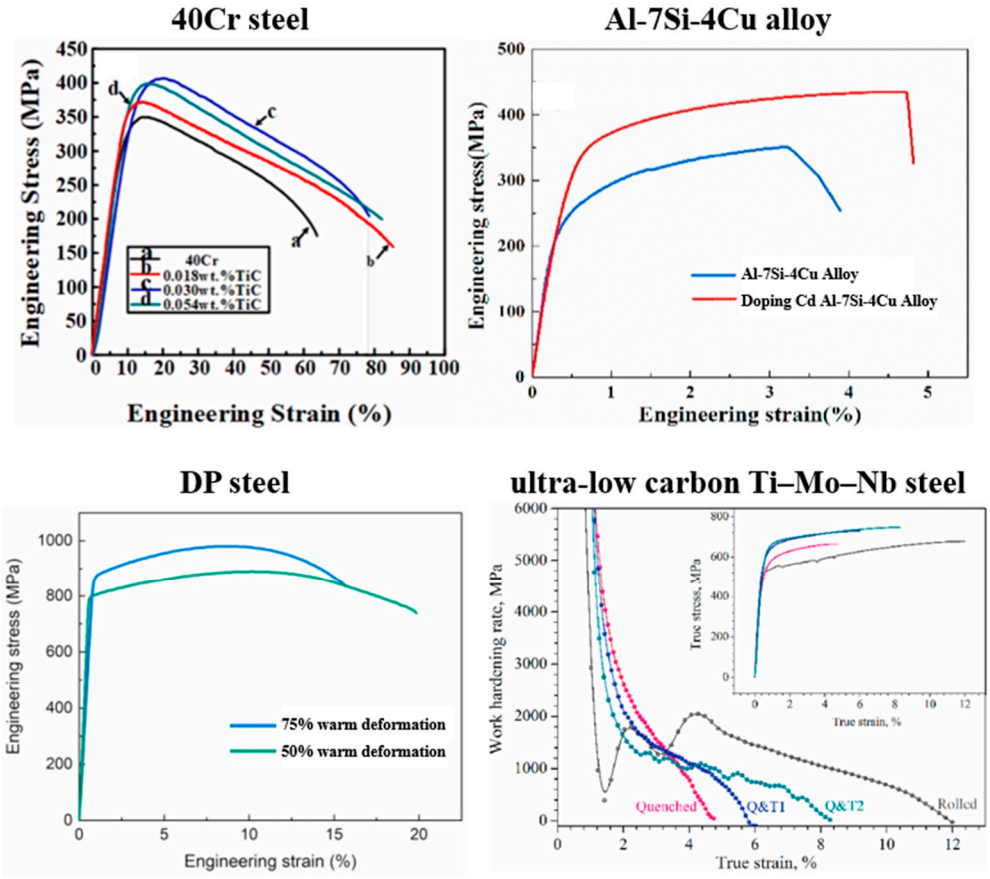


**Figure 13.** Engineering stress-strain curves/work hardening rate-true strain curves of metal materials with optimized properties. Reprinted with permission from ref. [42,45,48,106], Copyright 2022 Elsevier.

Therefore, the strengthening of metal materials is mainly attributed to fine grain strengthening, solution strengthening, and precipitation strengthening. However, strengthening by precipitate hardening, pining of dislocation by solute clustering and dislocation hardening raise yield strength without raising fracture toughness [86]. At the same time, when the relationship between the precipitates and the matrix changed from coherent to semi-coherent or incoherent, the strength deteriorated gradually [102]. It is well known that increasing the yield strength and fracture toughness simultaneously through refinement of grain size is a feasible solution [8]. In addition, according to the latest studies, for nanoparticles with coherent/semi-coherent interface relationship, when the moving dislocation interacts with the nanoparticles, part of them will pile up and others will continue to keep slipping along the coherent interface. This will not result in the aggregation and hindrance of dislocation; a schematic diagram is shown in Figure 14 [74]. Hence, the strength and toughness can be improved simultaneously by coherent/semi-coherent nanoparticles introduced into the metal matrix [64]. Experimentally, the in situ nanoparticles obtained by in situ nano-manufacturing technology have a coherent/semi-coherent relationship with metal matrix (Figure 14b) [71]. With in situ nanoparticles strengthened copper alloy [76] and Ni-Cr-Mo steel [69] can simultaneously enhance the strength and ductility, as shown in

Figure 14c,d, respectively. It should be noted that the tensile properties are obtained under static loading at room temperature.

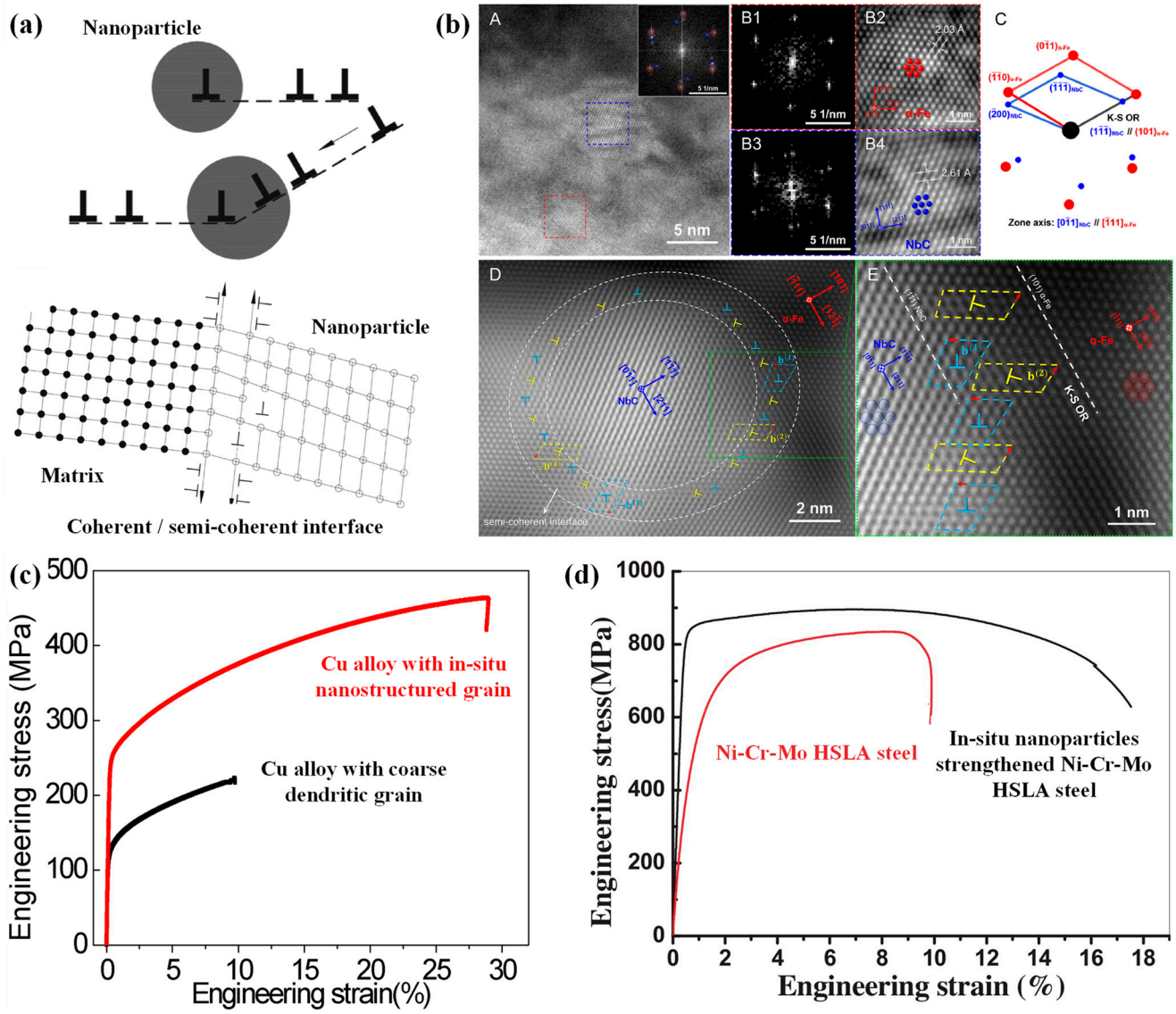


**Figure 14.** (**a**) Strengthening mechanisms of the nanoparticles being coherent/semi-coherent to the matrix, reprinted with permission from ref. [74], 2022, Elsevier; (**b**) misfit dislocation at a NbC/α-Fe semi-coherent interface alone the $[0\bar{1}0]_{NbC}//[\bar{1}11]_{\alpha-Fe}$ directions (A, HRTEM image of a typical NbC and the surrounding α-Fe; B1 (FFT) and B2 inversed FFT (IFFT) of α-Fe in the red square; B3 (FFT) and B4 (IFFT) of NbC in the blue square; C, Schematic summarizing the diffraction patterns for the orientation relationship (OR) between the NbC and α-Fe; D, NbC/α-Fe interface with high-density misfit dislocations; E, Enlarged image of the green dotted zone in D), reprinted with permission from ref. [71], 2022, Elsevier; (**c**) tensile engineering stress-strain curves of Cu alloy with/without in situ nanoparticles, reprinted with permission from ref. [76], 2022, Elsevier; (**d**) tensile engineering stress-strain curves of in situ nanoparticles strengthened HSLA steel and comparison steel, reprinted with permission from ref. [69], 2022, Elsevier.

A number of nanoparticles are embedded in the metal matrix grains, and the mechanism of simultaneously improving strength and ductility of nanostructured materials is as follows: (1) Nanoparticles have the effect of heterogeneous nucleation on the matrix to significantly refine the grain, second phase, and inclusion size during metal solidification and heat treatment [77,108]; (2) A huge number of nanoparticles homogeneously distributed in

the matrix grain result in overall high density and uniform distribution of dislocation during deformation; high dislocation density improves the ductility of crystalline metal [3,106]; (3) Through the formation of nanostructured grains, the formation of the hard brittle segregation phase and microporous defects is reduced, and the stability of mechanical properties is improved [4]; (4) coherent or semi-coherent interfaces between nanoparticles and matrix changes the dislocation pile-up style at the interface; it creates favorable condition for the dislocation slip through the interface, avoids dislocations piling up at the interface between particles and the matrix, and improves the plastic of metals [73,74].

## 5. Conclusions and Prospect

This review highlights the current progress in the fabrication technique, microstructure, and mechanical properties of metal-matrix nanostructured materials, such as steel, copper alloy, and aluminum alloy. The effect of different manufacturing technologies and processes on the microstructure and properties of metal materials were briefly covered. There is no doubt that the introduction of nanoparticles into the metal matrix by various methods has a significant impact on the microstructure and mechanism properties, especially the grain size and yield strength. However, in order to simultaneously improve strength and ductility of metal materials, it is necessary to introduce in situ nanoparticles with coherent or semi-coherent interfaces into the metallic matrix. The improvement of microstructure uniformity, such as grain refinement, inhibiting segregation, second phase, and inclusions refinement, is an important prerequisite for obtaining the property uniformity of metal materials. It should be mentioned that the strength and ductility of in situ nanoparticle strengthened materials is far from the limit. The development of computer-computing capabilities and first-principle calculation application will further optimize the composition and crystallographic structure of in situ nanoparticles and promote the further development of nanostructured materials. The improvement of property uniformity will further enhance the service life of metal materials, which has significance in achieving emission peaks and carbon neutrality.

**Author Contributions:** Conceptualization, Z.W. and J.Q.; methodology, X.C.; software, W.Z.; validation, Y.W. and M.C.; formal analysis, Z.W. and J.Q.; investigation, J.Q.; resources, Z.W. and X.C.; writing—original draft preparation, J.Q.; writing—review and editing, Y.Z. and S.P.; visualization, J.Q. and W.Z.; supervision, Y.W. and X.C.; project administration, Y.W.; funding acquisition, Y.W. All authors have read and agreed to the published version of the manuscript.

**Funding:** This work was supported by the National Natural Science Foundation of China (52071012 and 51971031), the Academic and Technical Leaders of Major Disciplines in Jiangxi Province (20182BCB22020), and the Central Funds Guiding the Local Science and Technology Develop-ment-Fundamental Research (YDZX2021005).

**Institutional Review Board Statement:** Not applicable.

**Informed Consent Statement:** Not applicable.

**Data Availability Statement:** Not applicable.

**Conflicts of Interest:** The authors have no conflict of interest to declare that are relevant to the content of this article.

## References

1. Dutta, R.K.; Petrov, R.H.; Delhez, R.; Hermans, M.J.M.; Richardson, I.M.; Böttger, A.J. The effect of tensile deformation by in situ ultrasonic treatment on the microstructure of low-carbon steel. *Acta Mater.* **2013**, *61*, 1592–1602. [CrossRef]
2. Zhou, P.S.; Wang, B.; Wang, L.; Hu, Y.W.; Zhou, L. Effect of welding heat input on grain boundary evolution and toughness properties in CGHAZ of X90 pipeline steel. *Mater. Sci. Eng. A* **2018**, *722*, 112–121. [CrossRef]
3. Chen, K.; Zhang, J.; Chen, X.; Wang, Z.; Shi, R.; Zhang, A. The effect of iron on the microstructure and mechanical properties of a cast Cu–12Sn-1.5Ni (wt.%) alloy. *Mater. Sci. Eng. A* **2020**, *785*, 139330. [CrossRef]
4. Liu, X.; Zhao, Q.L.; Ji, Z.W.; Wang, B.; Zhu, Y.L.; Jiang, Q.C. Effectively mitigated macro-segregation and improved tensile properties of twin-roll casting Al-Cu strips via the addition of TiC nanoparticles. *J. Mater. Process. Technol.* **2021**, *296*, 117200. [CrossRef]

5. Zhang, H.T.; Fu, H.D.; Zhu, S.C.; Yong, W.; Xie, J.X. Machine learning assisted composition effective design for precipitation strengthened copper alloys. *Acta Mater.* **2021**, *215*, 117118. [CrossRef]
6. Zhu, Y.; Chen, X.; Chen, K.; Wang, Y.; Wang, Z. Quasi in situ observation of twinning evolution during strain path change in magnesium alloy. *J. Mater. Res.* **2022**, *37*, 1125–1132. [CrossRef]
7. Ma, E.; Zhu, T. Towards strength–ductility synergy through the design of heterogeneous nanostructures in metals. *Mater. Today* **2017**, *20*, 323–331. [CrossRef]
8. Lu, K. Materials science. The future of metals. *Science* **2010**, *328*, 319–320. [CrossRef]
9. Hall, E.O. The Deformation and Ageing of Mild Steel: III Discussion of Results. *Proc. Phys. Soc. Sect. B* **1951**, *64*, 747–753. [CrossRef]
10. Shi, R.; Wang, Z.; Qiao, L.; Pang, X. Microstructure evolution of in-situ nanoparticles and its comprehensive effect on high strength steel. *J. Mater. Sci. Technol.* **2019**, *35*, 1940–1950. [CrossRef]
11. Martin, J.H.; Yahata, B.; Mayer, J.; Mone, R.; Stonkevitch, E.; Miller, J.; O'Masta, M.R.; Schaedler, T.; Hundley, J.; Callahan, P.; et al. Grain refinement mechanisms in additively manufactured nano-functionalized aluminum. *Acta Mater.* **2020**, *200*, 1022–1037. [CrossRef]
12. Tang, H.; Chen, X.; Luo, X.; Chen, M.; Wang, Z.; Zuo, L. Heterogeneous nucleation effect of in situ nanoparticles on the metal–matrix microstructure. *Mater. Lett.* **2014**, *137*, 455–459. [CrossRef]
13. Ebrahimi, M.; Shaeri, M.H.; Naseri, R.; Gode, C. Equal channel angular extrusion for tube configuration of Al-Zn-Mg-Cu alloy. *Mater. Sci. Eng. A* **2018**, *731*, 569–576. [CrossRef]
14. Muñoz, J.A.; Komissarov, A.; Avalos, M.; Bolmaro, R.E. Mechanical and microstructural behavior of a heterogeneous austenitic stainless steel processed by Equal Channel Angular Sheet Extrusion (ECASE). *Mater. Sci. Eng. A* **2020**, *792*, 139779. [CrossRef]
15. Jiang, Y.; Gu, R.C.; Peterlechner, M.; Liu, Y.W.; Wang, J.T.; Wilde, G. Impurity effect on recrystallization and grain growth in severe plastically deformed copper. *Mater. Sci. Eng. A* **2021**, *824*, 141786. [CrossRef]
16. Oh, J.; Park, S.; Bae, H.J.; Son, S.; Kim, H.S.; Seol, J.B.; Sung, H.; Kim, J.G. Mechanical properties and microstructural evolution of high-pressure torsion-processed Al7075 alloy at elevated temperatures. *Mater. Sci. Eng. A* **2022**, *835*, 142692. [CrossRef]
17. Jang, G.; Kim, J.N.; Lee, H.; Lee, T.; Enikeev, N.; Abramova, M.; Valiev, R.Z.; Kim, H.S.; Lee, C.S. Microstructural evolution and mechanical properties of nanocrystalline Fe–Mn–Al–C steel processed by high-pressure torsion. *Mater. Sci. Eng. A* **2021**, *827*, 142073. [CrossRef]
18. Manjunath, G.A.; Shivakumar, S.; Fernandez, R.; Nikhil, R.; Sharath, P.C. A review on effect of multi-directional forging/multi-axial forging on mechanical and microstructural properties of aluminum alloy. *Mater. Today Proc.* **2021**, *47*, 2565–2569. [CrossRef]
19. Haghdadi, N.; Zarei-Hanzaki, A.; Abou-Ras, D.; Maghsoudi, M.H.; Ghorbani, A.; Kawasaki, M. An investigation into the homogeneity of microstructure, strain pattern and hardness of pure aluminum processed by accumulative back extrusion. *Mater. Sci. Eng. A* **2014**, *595*, 179–187. [CrossRef]
20. Haghdadi, N.; Zarei-Hanzaki, A.; Abou-Ras, D. Microstructure and mechanical properties of commercially pure aluminum processed by accumulative back extrusion. *Mater. Sci. Eng. A* **2013**, *584*, 73–81. [CrossRef]
21. Rao, G.N.M.; Kumar, V.R.M. A review on recent advances in accumulative roll bonding of similar, dissimilar and metal matrix composites. *Mater. Today Proc.* **2022**, *56*, A13–A18. [CrossRef]
22. Meyers, M.A.; Mishra, A.; Benson, D.J. Mechanical properties of nanocrystalline materials. *Prog. Mater. Sci.* **2006**, *51*, 427–556. [CrossRef]
23. Fang, T.H.; Li, W.L.; Tao, N.R.; Lu, K. Revealing extraordinary intrinsic tensile plasticity in gradient nano-grained copper. *Science* **2011**, *331*, 1587–1590. [CrossRef]
24. Lu, K. Nanomaterials. Making strong nanomaterials ductile with gradients. *Science* **2014**, *345*, 1455–1456. [CrossRef]
25. Wu, X.; Jiang, P.; Chen, L.; Yuan, F.; Zhu, Y.T. Extraordinary strain hardening by gradient structure. *Proc. Natl. Acad. Sci. USA* **2014**, *111*, 7197–7201. [CrossRef]
26. Ghosh, S.; Bibhanshu, N.; Suwas, S.; Chatterjee, K. Surface mechanical attrition treatment of additively manufactured 316L stainless steel yields gradient nanostructure with superior strength and ductility. *Mater. Sci. Eng. A* **2021**, *820*, 141540. [CrossRef]
27. Olugbade, T.O.; Lu, J. Literature review on the mechanical properties of materials after surface mechanical attrition treatment (SMAT). *Nano Mater. Sci.* **2020**, *2*, 3–31. [CrossRef]
28. Zhou, X.; Li, X.; Lu, K. 70 nm: The most unstable grain size in Cu prepared by surface mechanical grinding treatment. *Nano Mater. Sci.* **2020**, *2*, 32–38. [CrossRef]
29. Long, J.; Pan, Q.; Tao, N.; Dao, M.; Suresh, S.; Lu, L. Improved fatigue resistance of gradient nanograined Cu. *Acta Mater.* **2019**, *166*, 56–66. [CrossRef]
30. Lei, Y.B.; Wang, Z.B.; Zhang, B.; Luo, Z.P.; Lu, J.; Lu, K. Enhanced mechanical properties and corrosion resistance of 316L stainless steel by pre-forming a gradient nanostructured surface layer and annealing. *Acta Mater.* **2021**, *208*, 116773. [CrossRef]
31. Mei, X.M.; Mei, Q.S.; Li, J.Y.; Li, C.L.; Wan, L.; Chen, F.; Chen, Z.H.; Xu, T.; Wang, Y.C.; Tan, Y.Y. Solid-state alloying of Al-Mg alloys by accumulative roll-bonding: Microstructure and properties. *J. Mater. Sci. Technol.* **2022**, *125*, 238–251. [CrossRef]
32. Edry, I.; Shoihet, A.; Hayun, S. On the effects of electric current intensity and pulse frequency on the solidified structure of pure aluminum subjected to pulse magneto-oscillation treatment. *J. Mater. Processing Technol.* **2021**, *288*, 116844. [CrossRef]

33. Vorontsov, A.; Astafurov, S.; Melnikov, E.; Moskvina, V.; Kolubaev, E.; Astafurova, E. The microstructure, phase composition and tensile properties of austenitic stainless steel in a wire-feed electron beam melting combined with ultrasonic vibration. *Mater. Sci. Eng. A* **2021**, *820*, 141519. [CrossRef]
34. Yang, Y.; Zhang, K.; Li, Y.; Feng, X.; Luo, T. Solidification Structure Control by the Interaction of Pulsed Magnetic Field and Melt. *Procedia Manuf.* **2019**, *37*, 621–626. [CrossRef]
35. Stephenson, P.L.; Haghdadi, N.; DeMott, R.; Liao, X.Z.; Ringer, S.P.; Primig, S. Effect of scanning strategy on variant selection in additively manufactured Ti-6Al-4V. *Addit. Manuf.* **2020**, *36*, 101581. [CrossRef]
36. Mostafaei, A.; Hilla, C.; Stevens, E.L.; Nandwana, P.; Elliott, A.M.; Chmielus, M. Comparison of characterization methods for differently atomized nickel-based alloy 625 powders. *Powder Technol.* **2018**, *333*, 180–192. [CrossRef]
37. Sun, L.; Liu, Y.; Li, J.; Chen, K.; Gao, Y.; Yang, G. Morphology and microstructure of Fe–Cr–W–B alloy powders prepared by argon gas atomization. *Vacuum* **2022**, *200*, 111046. [CrossRef]
38. Zhang, C.Y.; Yuan, G.; Zhang, Y.X.; Liu, C.Y.; Fang, F.; Wang, G.D.; Misra, R.D.K. Cu-based amorphous alloy plates fabricated via twin-roll strip casting. *Mater. Sci. Eng. A* **2021**, *828*, 142123. [CrossRef]
39. Fang, F.; Che, S.; Hou, D.; Zhang, Y.; Wang, Y.; Zhang, W.; Yuan, G.; Zhang, X.; Misra, R.D.K.; Wang, G. Thin-gauge non-oriented silicon steel with balanced magnetic and mechanical properties processed by strip casting. *Mater. Sci. Eng. A* **2022**, *831*, 142284. [CrossRef]
40. Geng, Y.; Ban, Y.; Li, X.; Zhang, Y.; Jia, Y.; Tian, B.; Zhou, M.; Liu, Y.; Volinsky, A.A.; Song, K.; et al. Excellent mechanical properties and high electrical conductivity of Cu-Co-Si-Ti alloy due to multiple strengthening. *Mater. Sci. Eng. A* **2021**, *821*, 141639. [CrossRef]
41. Gleiter, H. Nanostructured materials: Basic concepts and microstructure. *Acta Mater.* **2000**, *48*, 1–29. [CrossRef]
42. Cai, M.; Chen, L.; Fang, K.; Huang, H.; Hodgson, P. The effects of a ferritic or martensitic matrix on the tensile behavior of a nano-precipitation strengthened ultra-low carbon Ti–Mo–Nb steel. *Mater. Sci. Eng. A* **2021**, *801*, 140410. [CrossRef]
43. Lei, G.; Wang, B.; Lu, J.; Wang, C.; Li, Y.; Luo, F. Effects of solid solution temperature on the microstructure and properties of 6013 aluminum alloy. *Mater. Chem. Phys.* **2022**, *280*, 125829. [CrossRef]
44. Huang, C.Y.; Yen, H.W. HRTEM investigations on nano precipitates in Custom 475 maraging stainless steel. *Mater. Charact.* **2021**, *178*, 111216. [CrossRef]
45. Gao, X.; Wang, H.; Xing, L.; Ma, C.; Li, Y.; Sha, G.; Ren, H. The synergistic effects of ultrafine grains and nano-size Cu-rich precipitates on the mechanical properties of DP steels. *Mater. Sci. Eng. A* **2021**, *805*, 140547. [CrossRef]
46. Pan, S.; Chen, X.; Zhou, X.; Wang, Z.; Chen, K.; Cao, Y.; Lu, F.; Li, S. Micro-alloying effect of Er and Zr on microstructural evolution and yield strength of Al-3Cu (wt.%) binary alloys. *Mater. Sci. Eng. A* **2020**, *790*, 139391. [CrossRef]
47. Pereira, V.S.M.; Davis, T.P.; Mayoral, M.H.; Kumar, A.; Schut, H.; Sietsma, J. Investigation of coarsening of oxide nanoparticles at 1400 K and its effect on the microstructure formation of an ODS Eurofer steel. *Mater. Charact.* **2022**, *185*, 111723. [CrossRef]
48. Zhang, H.; Wang, W.X.; Chang, F.; Li, C.L.; Shu, S.L.; Wang, Z.F.; Han, X.; Zou, Q.; Qiu, F.; Jiang, Q.C. Microstructure manipulation and strengthening mechanisms of 40Cr steel via trace TiC nanoparticles. *Mat. Sci. Eng. A Struct.* **2021**, *822*, 141693. [CrossRef]
49. Yang, C.; Zhao, Q.; Zhang, Z.; Li, L.; Tian, W.; Liu, R.; Zhang, P.; Xu, Y.; Li, Y.; Zhang, Z.; et al. Nanoparticle additions promote outstanding fracture toughness and fatigue strength in a cast Al–Cu alloy. *Mater. Des.* **2020**, *186*, 108221. [CrossRef]
50. Li, X.P.; Ji, G.; Chen, Z.; Addad, A.; Wu, Y.; Wang, H.W.; Vleugels, J.; van Humbeeck, J.; Kruth, J.P. Selective laser melting of nano-$TiB_2$ decorated $AlSi_{10}Mg$ alloy with high fracture strength and ductility. *Acta Mater.* **2017**, *129*, 183–193. [CrossRef]
51. Martin, J.H.; Yahata, B.D.; Hundley, J.M.; Mayer, J.A.; Schaedler, T.A.; Pollock, T.M. 3D printing of high-strength aluminium alloys. *Nature* **2017**, *549*, 365–369. [CrossRef]
52. Chen, M.-W.; Jiang, H.; Wang, Y.-L.; Wang, Q.-S.; Wang, Z.-D. The effect of far-field uniform flow on the particle growth in an undercooled alloy melt. *J. Cryst. Growth* **2011**, *318*, 145–149. [CrossRef]
53. Chen, M.W.; Wang, Y.L.; Zhang, H.; Wu, L.Y.; Wang, Z.D. The interface morphology of a spherical crystal in the undercooled melt affected by a far-field uniform flow. *J. Appl. Phys.* **2011**, *109*, 103517. [CrossRef]
54. Chen, M.W.; He, G.W.; Chen, X.Y.; Wang, Z.D. Interfacial evolution of a spherical particle in a uniaximal straining flow. *Chin. Phys. B* **2012**, *21*, 106802. [CrossRef]
55. Chen, M.-W.; Liu, X.-M.; Yang, Z.-C.; Wang, Z.-D. The asymptotic solution of particle growth in the convective undercooled melt driven by a biaxial straining flow. *Acta Mech. Sin.* **2015**, *31*, 73–78. [CrossRef]
56. Gao, J.; Chen, M.; Wang, Z. Shape evolution of a spherical particle growing in supersaturated solution affected by straining flows. *Mod. Phys. Lett. B* **2016**, *30*, 1650059. [CrossRef]
57. Chen, M.; Liu, W.; Wang, Z. The asymptotic solution for the particle growth in the undercooled melt driven by a straining flow. *Mod. Phys. Lett. B* **2019**, *33*, 1950398. [CrossRef]
58. Chen, M.-W.; Wang, X.-F.; Wang, F.; Lin, G.-B.; Wang, Z.-Z. The effect of interfacial kinetics on the morphological stability of a spherical particle. *J. Cryst. Growth* **2013**, *362*, 20–23. [CrossRef]
59. Chen, M.; Ji, X.; Xu, X.; Zheng, Y.; Qian, P.; Wang, Z. The effect of the shear flow on particle growth in the undercooled melt. *J. Cryst. Growth* **2014**, *401*, 116–119. [CrossRef]
60. Chen, M.-W.; Mi, J.-X.; Wang, Z.-D. The effect of oscillatory flow on nucleation and grain growth in the undercooled melt. *J. Cryst. Growth* **2017**, *468*, 32–37. [CrossRef]

61. Chen, M.W.; Li, L.Y.; Guo, H.M. The dynamics of nucleation and growth of a particle in the ternary alloy melt with anisotropic surface tension. *J. Chem. Phys.* **2017**, *147*, 084707. [CrossRef]
62. Chen, M.W.; Wang, Y.X.; Guo, H.M. The effect of anisotropic surface tension on interfacial evolution of a particle in the binary alloy melt. *J. Cryst. Growth* **2019**, *510*, 32–39. [CrossRef]
63. Jiang, H.; Chen, M.W.; Wang, Z.D. Effect of Anisotropic Surface Tension on the Morphological Stability of Deep Cellular Crystal Growth in Directional Solidification. *Surf. Rev. Lett.* **2019**, *26*, 1850210. [CrossRef]
64. Tang, H.; Chen, X.; Chen, M.; Zuo, L.; Hou, B.; Wang, Z. Microstructure and mechanical property of in-situ nano-particle strengthened ferritic steel by novel internal oxidation. *Mater. Sci. Eng. A* **2014**, *609*, 293–299. [CrossRef]
65. Shi, R.; Tu, Y.; Gao, K.; Qiao, L.; Pang, X. High stress corrosion cracking resistance of in-situ nanoparticle strengthened steel. *Corros. Commun.* **2022**, *5*, 14–24. [CrossRef]
66. Pan, P.; Tang, H.; Chen, X.; Wang, Z.; Zuo, L.; Yang, M.; Cao, Y. Effects of direct-quenching and tempering on the microstructure and mechanical properties of an ultra-low carbon Ti containing bainite steel. *Mater. Sci. Eng. A* **2020**, *796*, 139987. [CrossRef]
67. Luo, X.; Xu, G.; Chen, X.; Wang, Z. Effect of undercooled austenite ausforming on the role of the M–A constituents in the CGHAZ toughness of the HSLA steels with bainite structure. *Mater. Sci. Eng. A* **2022**, *833*, 142571. [CrossRef]
68. Luo, X.; Wang, Z.; Chen, X.; Wang, Y.; Xu, G. Modifying of microstructure and toughness in the weld metal prepared by welding wire containing nanosized titanium oxides. *Mater. Sci. Eng. A* **2021**, *807*, 140897. [CrossRef]
69. Chen, X.; Qiu, L.; Tang, H.; Luo, X.; Zuo, L.; Wang, Z.; Wang, Y. Effect of nanoparticles formed in liquid melt on microstructure and mechanical property of high strength naval steel. *J. Mater. Process. Technol.* **2015**, *222*, 224–233. [CrossRef]
70. Niu, Y.; Tang, H.; Wang, Y.; Chen, X.; Wang, Z.; Chen, K.; Wu, Y.; Liu, X. Effect of In Situ Nano-Particles on the Microstructure and Mechanical Properties of Ferritic Steel. *Steel Res. Int.* **2016**, *87*, 1389–1394. [CrossRef]
71. Shi, R.; Ma, Y.; Wang, Z.; Gao, L.; Yang, X.-S.; Qiao, L.; Pang, X. Atomic-scale investigation of deep hydrogen trapping in NbC/α-Fe semi-coherent interfaces. *Acta Mater.* **2020**, *200*, 686–698. [CrossRef]
72. Wang, Z.; Wang, X.; Wang, Q.; Shih, I.; Xu, J.J. Fabrication of a nanocomposite from in situ iron nanoparticle reinforced copper alloy. *Nanotechnology* **2009**, *20*, 075605. [CrossRef]
73. Chen, X.H.; Wang, Z.D.; Ding, D.; Tang, H.; Qiu, L.L.; Luo, X.; Shi, G.D. Strengthening and toughening strategies for tin bronze alloy through fabricating in-situ nanostructured grains. *Mater. Des.* **2015**, *66*, 60–66. [CrossRef]
74. Shi, G.; Chen, X.; Jiang, H.; Wang, Z.; Tang, H.; Fan, Y. Strengthening mechanisms of Fe nanoparticles for single crystal Cu–Fe alloy. *Mater. Sci. Eng. A* **2015**, *636*, 43–47. [CrossRef]
75. Chen, K.; Chen, X.; Ding, D.; Shi, G.; Wang, Z. Crystallographic features of iron-rich nanoparticles in cast Cu–10Sn–2Zn–1.5Fe–0.5Co alloy. *Mater. Charact.* **2016**, *113*, 34–42. [CrossRef]
76. Chen, K.; Chen, X.; Ding, D.; Shi, G.; Wang, Z. Formation mechanism of in-situ nanostructured grain in cast Cu–10Sn–2Zn–1.5Fe–0.5Co (wt.%) alloy. *Mater. Des.* **2016**, *94*, 338–344. [CrossRef]
77. Chen, K.; Chen, X.; Ding, D.; Shi, G.; Wang, Z. Heterogeneous nucleation effect of in situ iron-rich nanoparticles on grain refinement of copper alloy. *Mater. Lett.* **2016**, *168*, 188–191. [CrossRef]
78. Chen, K.; Chen, X.; Ding, D.; Wang, Z. Effect of in-situ nanoparticle wall on inhibiting segregation of tin bronze alloy. *Mater. Lett.* **2016**, *175*, 148–151. [CrossRef]
79. Chen, K.; Tang, H.; Chen, X.; Ding, D.; Shi, G.; Wang, Z. Morphological instability of spherical nano iron-rich crystal in copper melt. *Mater. Lett.* **2016**, *172*, 125–127. [CrossRef]
80. Chen, K.; Pan, S.; Zhu, Y.; Cheng, Y.; Chen, X.; Wang, Z. In situ observations of crack propagation in as-cast Cu-1.5Fe-0.5Co (wt%) alloy. *Mater. Sci. Eng. A* **2017**, *706*, 211–216. [CrossRef]
81. Chen, K.; Chen, X.; Wang, Z.; Mao, H.; Sandström, R. Optimization of deformation properties in as-cast copper by microstructural engineering. Part I. microstructure. *J. Alloys Compd.* **2018**, *763*, 592–605. [CrossRef]
82. Chen, K.; Chen, X.; Wang, Z. Precipitates-interaction capture of nano-sized iron-rich precipitates during copper solidification. *Mater. Sci. Technol.* **2019**, *35*, 1028–1037. [CrossRef]
83. Chen, K.X.; Korzhavyi, P.A.; Demange, G.; Zapolsky, H.; Patte, R.; Boisse, J.; Wang, Z.D. Morphological instability of iron-rich precipitates in Cu Fe Co alloys. *Acta Mater.* **2019**, *163*, 55–67. [CrossRef]
84. Chen, K.; Pan, S.; Chen, X.; Wang, Z.; Sandström, R. Optimisation of deformation properties in as-cast copper by microstructural engineering. Part II. Mechanical properties. *J. Alloys Compd.* **2020**, *812*, 151910. [CrossRef]
85. Chen, K.; Wu, X.; Zhang, A.; Zhang, J.; Chen, X.; Zhu, Y.; Wang, Z. Development of wear resistant Cu-12Sn-1.5Ni alloy via minor addition of Fe during casting process. *Appl. Surf. Sci.* **2022**, *573*, 151623. [CrossRef]
86. Xie, Z.J.; Langelier, B.; Tsai, Y.T.; Shang, C.J.; Yang, J.R.; Subramanian, S.V.; Ma, X.P.; Wang, X.L. Characterization of nano-sized precipitation and dislocations and the correlation with mechanical properties of a low alloy TRIP-aided steel. *Mater. Sci. Eng. A* **2019**, *763*, 138149. [CrossRef]
87. Hou, W.; Liu, Q.; Gu, J. Nano-sized austenite and Cu precipitates formed by using intercritical tempering plus tempering and their effect on the mechanical property in a low carbon Cu bearing 7 Ni steel. *Mater. Sci. Eng. A* **2020**, *780*, 139186. [CrossRef]
88. Niu, M.C.; Yang, K.; Luan, J.H.; Wang, W.; Jiao, Z.B. Cu-assisted austenite reversion and enhanced TRIP effect in maraging stainless steels. *J. Mater. Sci. Technol.* **2022**, *104*, 52–58. [CrossRef]

89. Chen, C.-Y.; Chiu, P.-H.; Yang, Y.-L.; Liu, W.-S.; Chen, Z.-W.; Lin, Y.-H.; Kang, Y.-C. Insight on nano-sized precipitate-hardened Ti-Mo 11Cr-11Ni martensitic stainless steel: Experimental Evidence and Related Patents Investigation. *Mater. Today Commun.* **2022**, *31*, 103454. [CrossRef]
90. Jiang, S.; Wang, H.; Wu, Y.; Liu, X.; Chen, H.; Yao, M.; Gault, B.; Ponge, D.; Raabe, D.; Hirata, A.; et al. Ultrastrong steel via minimal lattice misfit and high-density nanoprecipitation. *Nature* **2017**, *544*, 460–464. [CrossRef]
91. Yang, M.; King, D.J.M.; Povstugar, I.; Wen, Y.; Luan, J.; Kuhn, B.; Jiao, Z.; Wang, C.; Wenman, M.R.; Liu, X. Precipitation behavior in G-phase strengthened ferritic stainless steels. *Acta Mater.* **2021**, *205*, 116542. [CrossRef]
92. Cautaerts, N.; Rauch, E.F.; Jeong, J.; Dehm, G.; Liebscher, C.H. Investigation of the orientation relationship between nano-sized G-phase precipitates and austenite with scanning nano-beam electron diffraction using a pixelated detector. *Scr. Mater.* **2021**, *201*, 113930. [CrossRef]
93. Zhou, Q.; Zhao, X.M.; Li, Z.; Cui, X.J. The Influence of Isothermal Holding Times on Microstructural Evolution of X90 Linepipe Steel. *Mater. Res.-Ibero.-Am. J.* **2019**, *22*, e20180605. [CrossRef]
94. Pereloma, E.V.; Kostryzhev, A.G.; AlShahrani, A.; Zhu, C.; Cairney, J.M.; Killmore, C.R.; Ringer, S.P. Effect of austenite deformation temperature on Nb clustering and precipitation in microalloyed steel. *Scr. Mater.* **2014**, *75*, 74–77. [CrossRef]
95. Xiong, Z.; Timokhina, I.; Pereloma, E. Clustering, nano-scale precipitation and strengthening of steels. *Prog. Mater. Sci.* **2021**, *118*, 100764. [CrossRef]
96. Xiong, R.; Peng, H.; Zhang, T.; Bae, J.W.; Kim, H.S.; Wen, Y. Superior strain-hardening by deformation-induced nano-HCP martensite in Fe–Mn–Si–C high-manganese steel. *Mater. Sci. Eng. A* **2021**, *824*, 141864. [CrossRef]
97. Li, Z.; Xiao, Z.; Jiang, Y.; Lei, Q.; Xie, J. Composition design, phase transition and fabrication of copper alloys with high strength and electrical conductivity. *Chin. J. Nonferrous Met.* **2019**, *29*, 2009–2049.
98. Wang, C.; Fu, H.; Zhang, H.; He, X.; Xie, J. Simultaneous enhancement of mechanical and electrical properties of Cu–Ni–Si alloys via thermo-mechanical process. *Mater. Sci. Eng. A* **2022**, *838*, 142815. [CrossRef]
99. Liao, W.; Yang, H.; Yi, C.; Zheng, J. Effect and mechanism of cold rolling and aging process on microstructure and properties of columnar grain C70250 copper alloy. *Mater. Sci. Eng. A* **2022**, *833*, 142577. [CrossRef]
100. Liao, W.; Liu, X.; Yang, Y. Relationship and mechanism between double cold rolling-aging process, microstructure and properties of Cu–Ni–Si alloy prepared by two-phase zone continuous casting. *Mater. Sci. Eng. A* **2020**, *797*, 140148. [CrossRef]
101. Li, J.; Ding, H.; Li, B.; Wang, L. Microstructure evolution and properties of a Cu–Cr–Zr alloy with high strength and high conductivity. *Mater. Sci. Eng. A* **2021**, *819*, 141464. [CrossRef]
102. Fu, S.; Liu, P.; Chen, X.; Zhou, H.; Ma, F.; Li, W.; Zhang, K. Effect of aging process on the microstructure and properties of Cu–Cr–Ti alloy. *Mater. Sci. Eng. A* **2021**, *802*, 140598. [CrossRef]
103. Liu, W.; Chen, X.; Ahmad, T.; Zhou, C.; Xiao, X.; Wang, H.; Yang, B. Microstructures and mechanical properties of Cu–Ti alloys with ultrahigh strength and high ductility by thermo-mechanical treatment. *Mater. Sci. Eng. A* **2022**, *835*, 142672. [CrossRef]
104. Yan, K.; Chen, Z.; Lu, W.; Zhao, Y.; Le, W.; Naseem, S. Nucleation and growth of Al3Sc precipitates during isothermal aging of Al-0.55 wt% Sc alloy. *Mater. Charact.* **2021**, *179*, 111331. [CrossRef]
105. Chen, K.; Wu, X.; Cao, Y.; Wang, Z.; Zhang, X.; Wu, C.; Chen, M. Enhanced strength and ductility in an Al–Cu–Li alloy via long-term ageing. *Mater. Sci. Eng. A* **2021**, *811*, 141092. [CrossRef]
106. Cao, Y.; Chen, X.; Wang, Z.; Chen, K.; Tang, W.; Pan, S.; Yang, X.; Qin, J.; Li, S.; Wang, Y. Effect of Cd micro-addition on microstructure and mechanical properties in ternary Al-Si-Cu alloy. *J. Alloys Compd.* **2021**, *851*, 156739. [CrossRef]
107. Pan, S.; Qian, F.; Li, C.; Wang, Z.; Li, Y. Synergistic strengthening by nano-sized α-Al(Mn,Fe)Si and Al3Zr dispersoids in a heat-resistant Al–Mn–Fe–Si–Zr alloy. *Mater. Sci. Eng. A* **2021**, *819*, 141460. [CrossRef]
108. Zhai, W.; Zhou, W.; Nai, S.M.L. Grain refinement and strengthening of 316L stainless steel through addition of TiC nanoparticles and selective laser melting. *Mater. Sci. Eng. A* **2022**, *832*, 142460. [CrossRef]
109. Doñate-Buendia, C.; Kürnsteiner, P.; Stern, F.; Wilms, M.B.; Streubel, R.; Kusoglu, I.M.; Tenkamp, J.; Bruder, E.; Pirch, N.; Barcikowski, S.; et al. Microstructure formation and mechanical properties of ODS steels built by laser additive manufacturing of nanoparticle coated iron-chromium powders. *Acta Mater.* **2021**, *206*, 116566. [CrossRef]
110. Huang, C.C.; Qi, L.; Chen, J.; Guan, R.; Ojo, O.A.; Wang, Z.G. Effect of TiC nanoparticles on the hot deformation behavior of AA7075 aluminum alloy. *Mater. Charact.* **2021**, *181*, 111508. [CrossRef]
111. Zhu, H.-W.; Xu, K.; Qin, S.; Xiao, F.-R.; Liao, B. Effect of heat treatment on microstructure and properties of 1045 steel modified with (NbTi)C nanoparticles. *Mater. Sci. Eng. A* **2018**, *728*, 175–182. [CrossRef]
112. Dou, P.; Sang, W.; Kimura, A. Morphology, crystal and metal/oxide interface structures of nanoparticles in Fe–15Cr–2W–0.5Ti–7Al–0.4Zr–0.5Y2O3 ODS steel. *J. Nucl. Mater.* **2019**, *523*, 231–247. [CrossRef]
113. Fu, J.; Davis, T.P.; Kumar, A.; Richardson, I.M.; Hermans, M.J.M. Characterisation of the influence of vanadium and tantalum on yttrium-based nano-oxides in ODS Eurofer steel. *Mater. Charact.* **2021**, *175*, 111072. [CrossRef]
114. Fu, J.; Brouwer, J.C.; Richardson, I.M.; Hermans, M.J.M. Effect of mechanical alloying and spark plasma sintering on the microstructure and mechanical properties of ODS Eurofer. *Mater. Des.* **2019**, *177*, 107849. [CrossRef]
115. Ukai, S. Oxide Dispersion Strengthened Steels. *Compr. Nucl. Mater.* **2012**, *4*, 241–271.
116. Wang, B.; Zhang, Y.; Qiu, F.; Cai, G.; Cui, W.; Hu, Z.; Zhang, H.; Tyrer, N.; Barber, G.C. Role of trace nanoparticles in manipulating the widmanstatten structure of low carbon steel. *Mater. Lett.* **2022**, *306*, 130853. [CrossRef]

117. Cao, Y.; Chen, X.; Wang, Z.; Chen, K.; Pan, S.; Zhu, Y.; Wang, Y. Synergistic influence of La and Zr on microstructure and mechanical performance of an Al-Si-Mg alloy at casting state. *J. Alloys Compd.* **2022**, *902*, 163829. [CrossRef]
118. Maruschak, P.; Konovalenko, I.; Chausov, M.; Pylypenko, A.; Panin, S.; Vlasov, I.; Prentkovskis, O. Impact of Dynamic Non-Equilibrium Processes on Fracture Mechanisms of High-Strength Titanium Alloy VT23. *Metals* **2018**, *8*, 983. [CrossRef]
119. Maruschak, P.; Bishchak, R.; Prentkovskis, O.; Poberezhnyi, L.; Danyliuk, I.; Garbinčius, G. Peculiarities of the static and dynamic failure mechanism of long-term exploited gas pipeline steel. *Adv. Mech. Eng.* **2016**, *8*, 1687814016641565. [CrossRef]
120. Wang, P.; Wang, B.; Liu, Y.; Zhang, P.; Luan, Y.; Li, D.; Zhang, Z. Effects of inclusion types on the high-cycle fatigue properties of high-strength steel. *Scr. Mater.* **2022**, *210*, 114232. [CrossRef]